Reconstitution of a Juxtacrine Signaling Pathway by DNA-Programmed Cell Assembly

Bachelor Thesis 2

Submitted in fulfillment of the requirements for the degree of

"Bachelor of Science and Engineering"

Study Program:

"Engineering, Environmental and Biotechnology"

Management Center Innsbruck

Assessor:

Prof. Dr. Christoph Griesbeck

Author:

Mag. Matthias Lachner

MANAGEMENT CENTER INNSBRUCK

6020 Innsbruck / Austria, Egger-Lienz-Straße 120
+43 512 2070 3800, office-uvbt@mci.edu, www.mci.edu

Declaration in lieu of oath

I hereby declare, under oath, that this bachelor thesis has been my independent work and has not been aided with any prohibited means. I declare, to the best of my knowledge and belief, that all passages taken from published and unpublished sources or documents have been reproduced whether as original, slightly changed or in thought, have been mentioned as such at the corresponding places of the thesis, by citation, where the extent of the original quotes is indicated.

The paper has not been submitted for evaluation to another examination authority or has been published in this form or another.

San Francisco, CA, USA, 13/08/2010 _____

Abstract

Cell signaling processes provided the basis for the evolutionary transition from unicellular to multicellular organisms. A highly coordinated system of inter-cell communication is needed to govern the behavior of cells according to their respective microenvironment in an organism. This important function of cellular information processing implies that errors in cell signaling can constitute potential threats to the organization of the organism. Diseases like cancer, autoimmunity, or diabetes originate in such malfunctions. Understanding the mechanisms underlying the regulation of cell-cell signaling can help to find effective treatment for such diseases. Emulating cell communication processes *in vitro* allows for controlled investigation of these processes but is often difficult or impossible to achieve.

The DNA programmed approach of assembling single cells into complex 3D structures provides a novel method for the creation of microtissues and the study of cell-cell communication. By functionalizing cell surfaces of different cell types with short complementary single stranded oligonucleotides, assembly of defined multicellular three dimensional (3D) structures can be achieved. The reconstitution of a paracrine signaling pathway via DNA-mediated cell assembly was recently reported by Gartner and Bertozzi [1]. The aim of my project in the Gartner research group at the University of California, San Francisco, was to prove the applicability of this novel tool for studying juxtacrine signal transduction. The subject of investigation was the epidermal growth factor receptor (EGFR) pathway, stimulated by the transforming growth factor-α (TGFα). Studying of this pathway has a direct application in cancer research as both, ligand and receptor, are often overexpressed in human carcinomas. In order to reconstruct this pathway, I constructed two different cell lines expressing either ligand or receptor. Naturally the EGFR pathway operates through autocrine, paracrine, and juxtacrine modes of signaling. By presenting various combinations of elements of the pathway in controlled 3D microenvironments I aimed to tease apart the contribution of each mode towards overall EGFR signaling. Once assembled, receptor activation as a result of DNA programmed cell-cell interactions was monitored. Cells expressing the receptor were stimulated with soluble ligand or by co-culturing with ligand-expressing cells, representing either the paracrine or the juxtacrine signaling mode. Results demonstrate that cell surface modifications have no significant influence on receptor activation motivating future functional assays for the study of the EGFR-TGFα signaling mechanism using DNA-mediated assembly of 3D cellular microenvironments.

After a general introduction I will provide important theoretical aspects of functionalizing cell surfaces with DNA oligonucleotides, of TGFα and its receptor EGFR, and the differentiation between the paracrine and juxtacrine mode of cell signaling. After a section dealing with basic experimental procedures, I will present results of my experiments which indicate that the intensity of the EGFR signaling pathway is in some part dictated by the spatial mode through which it signals. Concluding remarks and future perspectives are provided in the last section.

Kurzfassung

Zellsignale waren ein wichtiger Schlüsselfaktor für den Übergang von einzelligen zu vielzelligen Organismen. Es bedarf eines hoch koordinierten Zusammenspiels verschiedenartiger Kommunikationswege um Zellen in ihren unterschiedlichen Mikroumgebungen in einem Organismus zu steuern. Diese wichtige Funktion von Zellsignalen impliziert jedoch gleichzeitig, dass Fehler in der Kommunikation fatale Folgen haben können. Krankheiten wie Krebs, Autoimmunität und Diabetes haben einen derartigen Ursprung und die Erforschung der Mechanismen, welche zu solchen Fehlkommunikationen führen, ist ausschlaggebend für die Entwicklung von effektiven Behandlungsmethoden. Die Nachahmung von Zellsignalwegen *in vitro* kann wesentlich zu unserem Verständnis beitragen, ist jedoch oft nur sehr schwer oder sogar unmöglich zu erreichen.

Mit dem Ziel diese Mängel zu beseitigen haben Prof. Zev J. Gartner und Kollegen eine Methode entwickelt, welche es erlaubt mit an Zelloberflächen befestigten komplementären Oligonukleotiden definierte dreidimensionale Zellstrukturen zu bilden. Das Ziel meines Projekts in der Forschungsgruppe von Prof. Gartner an der University of California, San Francisco, war einen bestimmten Signalweg in mit dieser Methode geformten, so genannten Mikrogeweben, zu untersuchen. Die Nachahmung eines parakrinen Signalmechanismus ist Gartner und Bertozzi bereits gelungen [1]. Ich widmete meine Forschung der Aktivierung des "epidermal growth factor receptor" (EGFR) durch einen seiner Liganden, "transforming growth factor-α" (TGFα). In natürlicher Umgebung erfolgt die Kommunikation durch diesen Signalweg in autokriner, parakriner und juxtakriner Weise. Ich beschäftigte mich allerdings vor allem mit der Möglichkeit den juxtakrinen Anteil unter Anwendung der DNA vermittelten Zellaggregation möglichst isoliert zu untersuchen. Die Anwendbarkeit dieser neuartigen Methode zur Erforschung eines juxtakrinen Signalweges sollte damit überprüft werden.

Um dies zu erreichen konstruierte ich zunächst Zelllinien, welche entweder nur EGFR oder TGFα exprimieren. Durch den Nachweis des Levels von durch Aktivierung phosphorylierten EGFR, in durch DNA vermittelten Zellaggregationen von TGFα und EGFR exprimierenden Zellen, konnte ich zeigen, dass keine signifikanten Unterschiede zur Kontrollgruppe, bestehend aus den gleichen Zellen, jedoch ohne Zelloberflächenmodifizierungen, zu erkennen waren. Diese Resultate motivieren zu zukünftigen Experimenten zur Erforschung dieses Signalweges.

In dieser Diplomarbeit werde ich nach einer allgemeinen Einleitung zunächst wichtige theoretische Aspekte der Funktionalisierung von Zelloberflächen mit DNA-Oligomeren, des Wachstumsfaktors TGFα, des EGF-Rezeptors und der Differenzierung von parakrinem und juxtakrinem Signalmechanismus erläutern. Danach folgt eine Beschreibung der experimentellen Prozeduren, des verwendeten Materials und der Methoden. Im nächsten Kapitel werden dann die Resultate der durchgeführten Experimente präsentiert und diskutiert. Diese Arbeit endet

schließlich mit abschließenden Bemerkungen und Vorschlägen für zukünftige Untersuchungen und Experimente.

Table of Contents

1 Introduction

The behavior of cells in multicellular organisms differs in accordance with their physical position within their respective microenvironments. A stem cell niche, for example, maintains stem cells in an undifferentiated state by providing a microenvironment containing secreted factors, extracellular matrix components, and cell-to-cell contacts. Culturing stem cells outside their niche contributes to differentiation. Similarly, it has been shown that two-dimensional (2D) *in vitro* studies of breast epithelial cells outside their normal microenvironment does not accurately mimic the complex interplay of cells found in the human mammary gland where they participate in complex interactions with other differentiated cell types within a defined, three-dimensional (3D) architecture [2]. However, recapitulating these interactions *in vitro* has proven challenging. To address these shortcomings, Prof. Zev J. Gartner and colleagues developed a novel method for templating the physical association among cells. By functionalizing cell membranes of different cell types with complementary short oligonucleotides, 3D structures with defined cell-to-cell contacts can be assembled.

The programmed assembly of cells into 3D living tissues holds the potential to revolutionize the way we study cell-cell interactions *in vitro*. Generally, the method provides controlled environments to study numerous juxtacrine signaling pathways with relevance to human health and disease. More specifically, the Gartner research group is using this approach to understand the effect of tissue structure on particular signaling pathways in breast cancer. My assignment was to perform critical proof-of-principle experiments to show the effects this method of assembly has on a particular signaling pathway. This strategy for assembling tissues is likely to impact other areas as well. For example, the behavior of stem cells may be altered via specific physical association with stromal cells, thereby facilitating self-renewal or directed differentiation into a variety of tissue types for the purpose of regenerative medicine. Potential advantages of DNA-programmed tissue assembly over other methods include the short period of time needed to assemble cells, the combinatorial means by which various cell types can be assembled, and the precision with which complex 3D architectures can be formed.

The aim of my project in the Gartner lab was to study activation of the human epidermal growth factor receptor (EGFR, also known as ErbB-1) by the transforming growth factor alpha (TGFα), a member of the epidermal growth factor (EGF) superfamily. Ligand binding to EGFR activates the receptor's internal tyrosine kinase domain and leads to phosphorylation of specific tyrosines in the cytoplasmic region. Changes in expression or activation of EGFR are common in many epithelial tumors [3]. Similarly, TGFα regulates cell growth and differentiation and is also widely expressed in malignant cancer, including breast cancer [4]. TGFα is typically cleaved from its transmembrane precursor allowing ligand binding to EGFR in a paracrine and autocrine fashion. However, experiments have shown that reduced ectodomain shedding in tumorigenic cells leads to juxtacrine EGFR activation with an increased efficiency relative to more typical paracrine signaling. On the one hand this may lead to a growth advantage for

malignant cells over normal cells [5]. On the other hand, high TGFα induced signaling beyond a certain threshold level, as observed in juxtacrine signaling assays, can lead to growth arrest [6]. Although not unambiguous, downregulation of CD9, a transmembrane tetraspanin which binds to TGFα on the cell surface and prevents it from cleavage, thereby increasing juxtacrine signaling levels which can lead to growth inhibition and decreased motility, has been associated with a poor prognosis of several carcinoma types in humans, including breast cancer [6, 7].

These observations demonstrate that differential modes of cell-cell signaling through the same molecule can lead to different stimulatory responses. Differentiating between juxtacrine, paracrine, and autocrine mediated responses to a given signaling molecule has the potential to unravel persistent questions and to provide insights into numerous cell-signaling processes. This, in turn, requires new methods capable of mimicking more structurally defined collections of cells – the goal of the programmed assembly strategy.

DNA templated tissue synthesis was previously demonstrated to facilitate paracrine signaling processes between different cell types [1]. The reconstitution of the TGFα-EGFR signaling pathway *in vitro* by DNA templated tissue synthesis is a first attempt to apply this novel method to study juxtacrine cell-cell communication. The primary aim of this work is to confirm its applicability to the study of this specific signaling mode. To do so, I first constructed stably transfected cell lines expressing either TGFα and EGFR in a null background by cloning the respective genes into an appropriate retroviral plasmid, generating retrovirus, and subsequently infecting 32D cells (a mouse hematopoietic progenitor cell line) or CHO cells (Chinese Hamster Ovary cells), respectively. In a second step I investigated juxtacrine activation of EGFR in 32D cells by applying Prof. Gartner's method of cell assembly. Generally this can be done in three different ways either by (i) direct modification of cell surface proteins by *N*-hydroxysuccinimide (NHS)-DNA conjugates [8], (ii) by copper-free click chemistry with difluorinated cyclooctyne (DIFO)-conjugated DNA of cells metabolically labeled with *N*-azidoacetylmannosamine [9], and (iii) by incubating cells with lipid-DNA conjugates, a new method currently being developed by the Gartner research group. My experiments were confined to surface modification with *N*-hydroxysuccinimide as this method has several advantages and is well established. The efficiency of cell-cell attachments were investigated by epifluorescence microscopy and flow cytometry. Activation of EGFR was measured by western blot with an anti phospho-EGFR antibody.

In the following chapters I will first provide important details of the assembly method, the TGFα ligand, its receptor EGFR, and the function and putative importance of juxtacrine signaling (chapter 2). In chapter 3, general experimental procedures will be explained. In chapter 4 I will then present and discuss the results. In chapter 5 I will draw final conclusions and give possible future directions.

2 Theoretical Background

2.1 *Cell Surface Labeling with DNA Oligonucleotides*

In the past decade several strategies have been developed to modify cell surfaces with different functional groups to achieve defined conjugates to cell surface components and thereby providing new tools for the study of cell biology, the control of stem cell differentiation, and the engineering of new tissues [8]. A recent approach is to covalently link single stranded DNA (ssDNA) oligomers to cell surfaces. DNA is biocompatible, easy to synthesize, and highly selective in its interactions with complementary strands. Hybridization with complementary oligonucleotides forms a strong yet reversible non-covalent bond. Further, the kinetics of hybridization can be easily controlled by altering DNA sequence [1].

Three different methods of labeling cell surfaces with ssDNA are commonly used by the Gartner research group. First, ssDNA covalently linked to a difluorinated cyclooctyne (DIFO) reagent can be reacted with azides displayed on glycans on living cell surfaces [10]. This method is described by the term "click chemistry" which emphasizes the rapid and specific character of the reaction under mild conditions [11]. Labeling of cells is achieved by incubation of cells with peracetylated *N*-azidoacetylmannosamine (Ac_4ManNAz) for three days. The azidosugar is metabolized to azido sialic acid residues and incorporated into cell surface glycans. DIFO conjugated ssDNA can then be reacted with cell surface azides. Figure 1 depicts the scheme for labeling cell surfaces with DIFO conjugates.

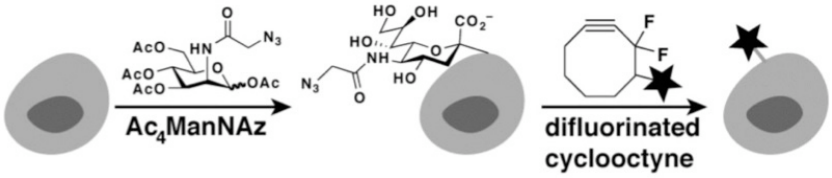

Figure 1. Labeling of cell surface glycans with azido sugars and DIFO reagents [10].

The second method, constituting the method of choice in this thesis, involves the attachment of succinimidyl-[(*N*-maleimidopropionamido)-hexaethyleneglycol] ester (NHS-PEG_6-maleimide) conjugated DNA (NHS-DNA) to amino groups of cell surface proteins [8]. Figure 2 illustrates the labeling process. First, thiolated ssDNA is chemically synthesized. Reaction with NHS-PEG_6-maleimide yields NHS-conjugated DNA, which can react with amino groups of cell surface lysines under conditions that do not disrupt the cell integrity. The most crucial advantage of NHS-DNA labeling is the short time needed to complete the labeling process. As no prolonged cell culture is required prior to cell surface labeling, the whole process can be accomplished in less than one hour. This makes the method more suitable for use with primary cells. Furthermore, all required reagents can be easily produced from commercially available starting materials.

One possible negative aspect of this particular chemical modification of a cell's surface might be its interference with surface proteins, especially with receptors that require strict conditions for ligand binding. Depending on the application, this interference could alter the results of the underlying research. This aspect raises the need to investigate the effects of cell surface modifications on protein functions, such as cell signaling, cell attachment, or migration capacity.

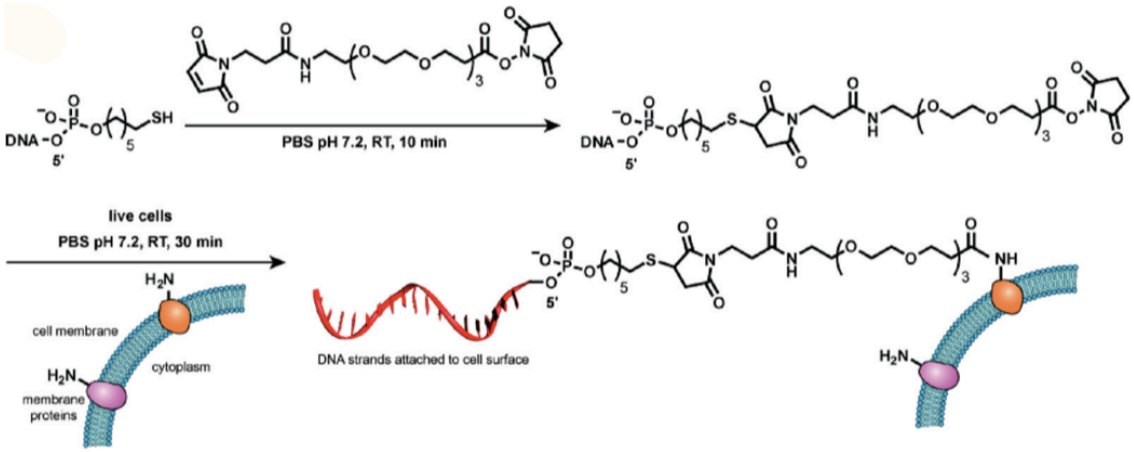

Figure 2. Graphic depiction of NHS-DNA labeling process of cell surface protein [8].

A novel third means of modifying cell surfaces with DNA is via incorporation of lipids attached to ssDNA molecules into the cell's membrane. This method is still in development and will not be described in detail. In brief, lipid-DNA conjugates are prepared synthetically. By incubation of cells with lipid-DNA, the hydrophobic lipidic portion of the conjugate is incorporated into the cell membrane while leaving the ssDNA exposed on the surface. The major advantage of this approach is the absolute control of the distance at which two cell membranes approach one another by controlling the length of the DNA strands or PEG linkers used in the conjugates. This cannot be achieved with the other methods as the DNA-conjugates react at random places on different cell surface proteins. Furthermore the reaction does not modify existing proteins, thus ensuring less interference with their function.

2.2 Transforming Growth Factor-α

The 50-amino acid TGFα polypeptide was first detected in conditioned media of several sarcoma virus transformed cells [12] but it is also expressed in many tumor derived cells and by embryos during early fetal development [13]. It interacts with the epidermal growth factor receptor (EGFR), thereby inducing activation of downstream signals such as the MAPK (Mitogen Activated Protein Kinase) pathway and to a less extent, the JAK/STAT (Signal Transducer and Activator of Transcription) pathway [4, 14, 15].

TGFα is a member of the epidermal growth factor (EGF) superfamily, a small group of structurally related growth factors. The first isolated and biochemically investigated member of this group was EGF itself [16, 17]. The group is characterized by a conserved amino acid sequence containing 6 cysteins over a sequence of 35-40 amino acids. These cysteins form disulfide bonds at known positions (Figure 3) [18, 19]. Other proteins not belonging to the EGF family and exhibiting different functions also contain this EGF motif. Notch receptors for example comprise as many as 36 EGF-like repeats [20], whereas TGFα as well as EGF only contain one.

The human TGFα mRNA sequence encodes a 160 amino acid transmembrane precursor starting with a 22-amino acid N-terminal signal sequence which is proteolytically cleaved from the rest of the protein post-translationally [21]. This signal sequence is followed by 17 amino acids containing an N-linked glycosylation site and carrying O-linked carbohydrates [13, 22]. This part is also referred to as the proTGFα region and is rapidly cleaved in certain cell types ($t_{1/2} \approx 15$ min in transfected CHO cells) [19]. The following 50 amino acids constitute the actual mature TGFα which is capable of binding and activating EGFR (bold line in Figure 3). The mature form of TGFα is then cleaved at its C-terminal side by TACE, a membrane-associated metalloprotease (also known as ADAM17) and released into the extracellular space, a process called ectodomain shedding [23]. Beyond a 9 amino acid long linker sequence another cleavage site can be found, followed by a hydrophobic 23-amino acid transmembrane region and a 39-amino acid C-terminal palmitoylated cytoplasmic sequence [13, 22].

Experiments with TGFα-transfected CHO cells show that cleavage at one of the two protease sites located C-terminal of the 50-amino acid TGFα sequence occurs at a very slow rate ($t_{1/2} \approx 4$ h) [19]. This leads to accumulation of proTGFα at the cell surface and the slow release of the mature 6 kDa 50-amino acid peptide into the media. In other experiments however, two larger forms (17 to 19 kDa) of soluble TGFα were found in the conditioned media of retrovirally transduced cells and tumor-derived cells, containing the N-glycosylated proTGFα sequence with or without the 9 amino-acid linker sequence on the C-terminal side of TGFα in [24, 25]. This finding suggest a faster cleavage at the C-terminal protease sites in those cells.

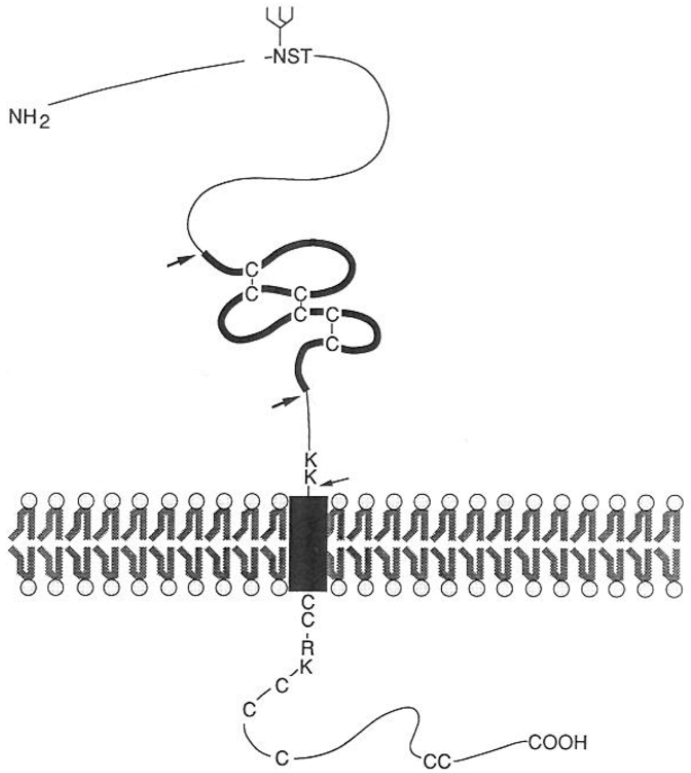

Figure 3. Graphical depiction of the TGFα precursor. The N-terminal signal peptide is cleaved and followed by an N-glycosylated proregion. The bold line depicts the mature 50-amino acid TGFα peptide with its cystein disulfide bonds. The transmembrane region (black box) is preceded by a short linker and followed by a cystein-rich cytoplasmic domain. This graphic was adapted from Derynck (1992) [22].

However, all examined TGFα synthesizing cells also exhibit uncleaved transmembrane precursors at the cell surface, and some do not secret TGFα into the medium at all [22]. Studies have shown that this membrane-bound precursor, also termed proTGFα, is able to activate EGFR in neighboring cells [21, 26]. To describe this mode of contact-dependent cell-cell signaling, the term "juxtacrine" has been introduced by Anklesaria et al. (1990) [27].

2.3 The Epidermal Growth Factor Receptor

The epidermal growth factor receptor EGFR, also referred to as HER1 (human EGF receptor) or ErbB1, is a 170 kDa transmembrane glycoprotein and is one of four members of the receptor tyrosine kinase (RTK) ErbB receptor family. Other family members are termed ErbB2, ErbB3, and ErbB4. All ErbB receptors are characterized by a large extracellular ligand binding domain (ca. 620 amino acids), a single transmembrane α-helix, a juxtamembrane region (ca. 45 amino acids), an intracellular tyrosine kinase domain (ca. 270 amino acids) and a C-terminal regulatory region (ca. 230 amino acids) containing multiple tyrosine residues which are subject to phosphorylation by the receptors intrinsic tyrosine kinase activity [3, 28-30]. Figure 4 depicts the domains of EGFR.

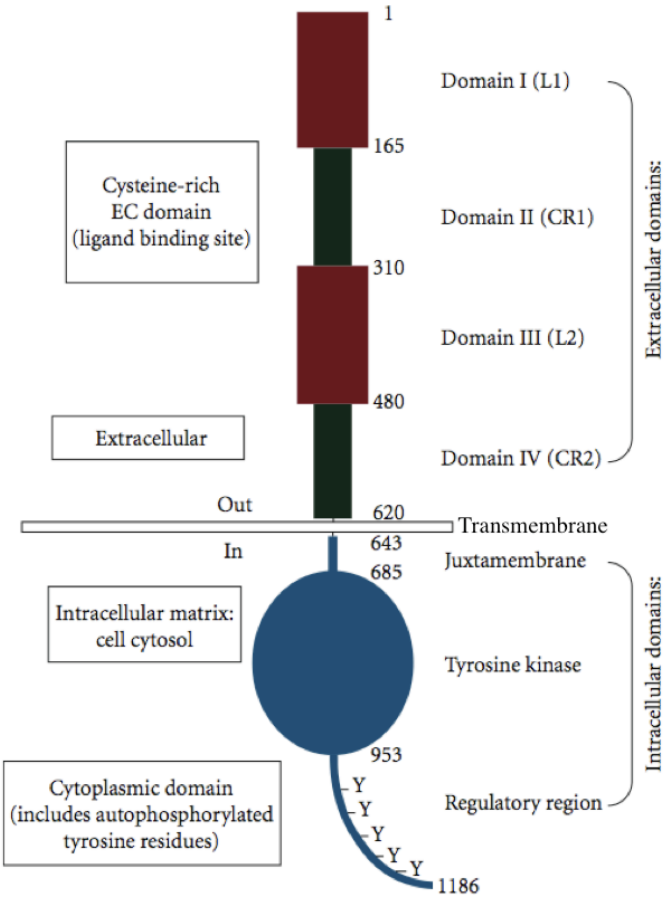

Figure 4. EGFR domain organization. The extracellular region consists of four domains. Domain I and III (or L1 and L2) are the ligand binding domains, domain II and IV (or CR1 and CR2) are cystein rich regions. A transmembrane helix is followed by a juxtamembrane region, the tyrosine kinase domain and a C-terminal regulatory region. Residue numbers indicate domain boundaries. The picture was slightly adapted from Flynn et al., 2009 [31].

Known mammalian EGFR ligands include EGF, TGFα, heparin-binding EGF-like growth factor (HB-EGF), amphiregulin (AR), betacellulin (BTC), epiregulin (EPR), and epigen [18]. Following ligand binding, EGFR monomers become prone to form homo- or heterodimers with itself or its ErbB family members resulting in activation of the tyrosine kinase domain and autophosphorylation. Although the ligands are bivalent, this mechanism does not require the ligand to act as a crosslinker between two receptor molecules as it was once believed. Analysis of EGFR crystal structures with bound TGFα and EGF ligands rather show that the ligand links the two EGFR ligand binding domains L1 and L2 of one single receptor molecule which leads to a dramatic conformational change of the extracellular region, unmasking a dimerization arm in domain II [32-34]. The dimerization of EGFR is therefore only "ligand-induced" but "receptor-mediated" [35]. Figure 5 shows the ligand-induced conformational changes of the extracellular EGFR region triggered by binding of EGF to the L1 and L2 domain.

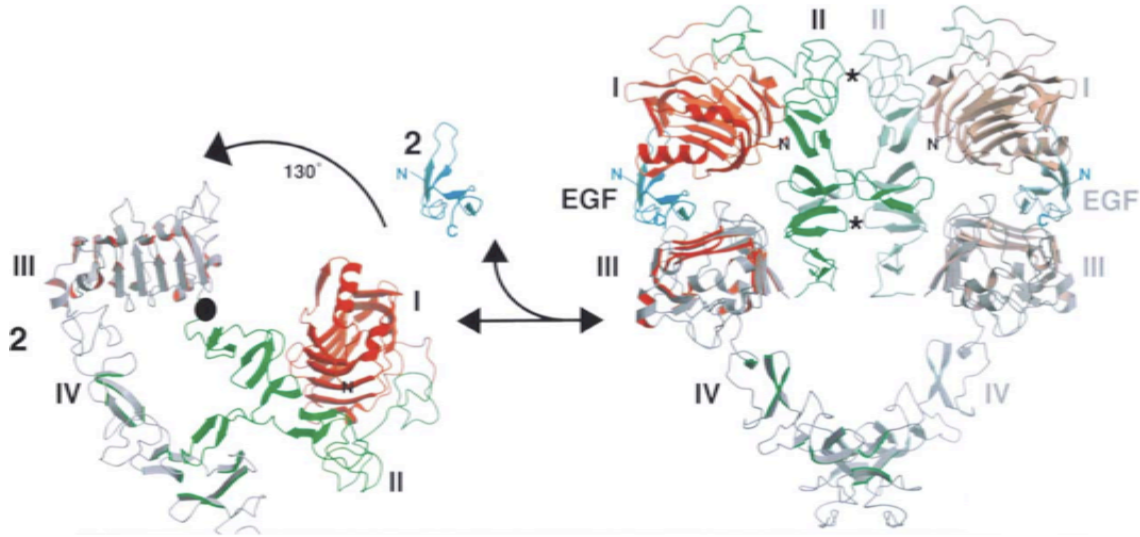

Figure 5. Structural changes of the EGFR extracellular region caused by binding of the EGF to the receptor (Burgess et al., 2003 [29]). Two receptor monomers and two EGF ligands form a heterooligomer. Domains I and II (CR1 and L1) form a rigid body which is proposed to rotate 130° about the axis labeled as black spot when autoinhibition by binding of domain II with domain IV is interrupted and the ligand binds.

Figure 6 describes the mechanism of ligand-induced dimerization and receptor activation. The same region in the cystein rich domain II which comprises the dimerization arm makes intramolecular interactions with domain IV, thereby forming a "tethered" configuration (Figure 6 A) [36]. It is generally believed that dimerization of receptor monomers is inhibited in this conformation [37]. It is also believed that this tethered conformation is in equilibrium with an "extended" conformation which exhibits higher ligand binding affinity [38, 39], as it was shown that mutations inhibiting the tethered configuration increase EGF binding affinity (Figure 6 B) [36]. It also appears likely that this allosteric activation of the EGF receptor is able to form dimers even in the absence of a ligand. However, ligand binding stabilizes the extended receptor structure resulting in exposure of the dimerization arm, thus promoting dimerization with other ligand-bound receptors (Figure 6 C and D) [28].

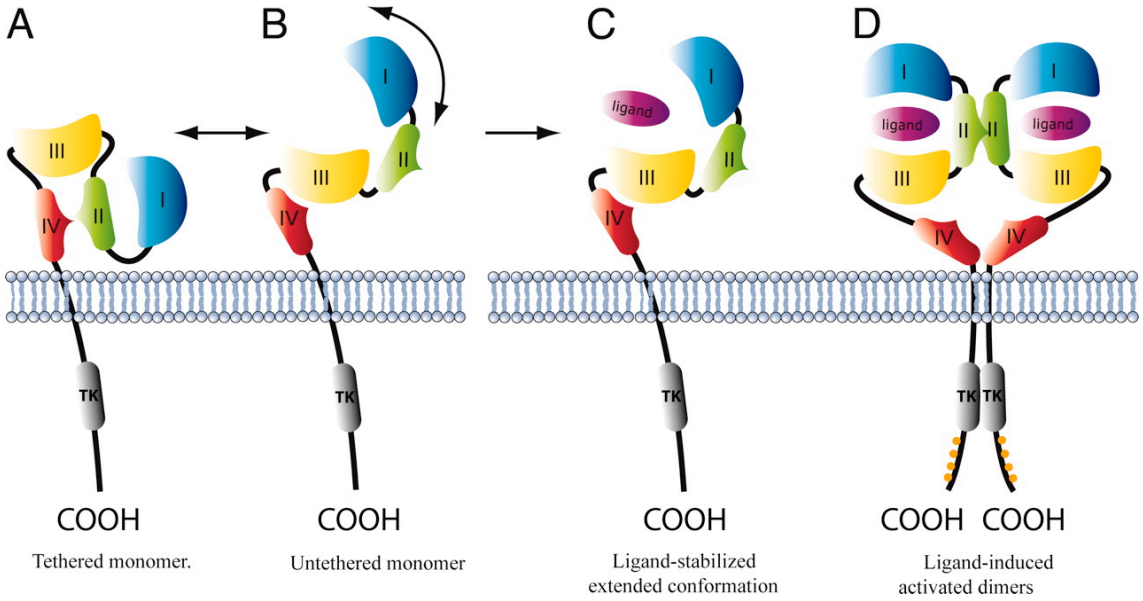

Figure 6. A proposed mechanism of ErbB/EGFR activation (Lammerts van Bueren et al., 2008) [40].

Dimerization activates the endogenous tyrosine kinase which leads to autophosphorylation in *trans* of various tyrosines residues on the cytoplasmic C-terminal tail. The exact mechanism of tyrosine kinase autoinhibition and its release is still not fully understood. One recent model suggests electrostatic binding of the protein tyrosine kinase and the juxtamembrane region to acidic lipids in the cell membrane restricts access of the kinase to its substrate tyrosine residues [41]. It is postulated that receptor dimerization leads to partial *trans* autophosphorylation which results in an increase of Ca^{2+} levels via the PLC-γ signaling pathway and activation of calmodulin (calcium modulated protein). Calmodulin then binds the EGFR juxtamembrane region, changes the local net charge, and releases the intracellular region from the membrane. This allows the formation of an asymmetric dimer of the two protein tyrosine kinase domains [42].

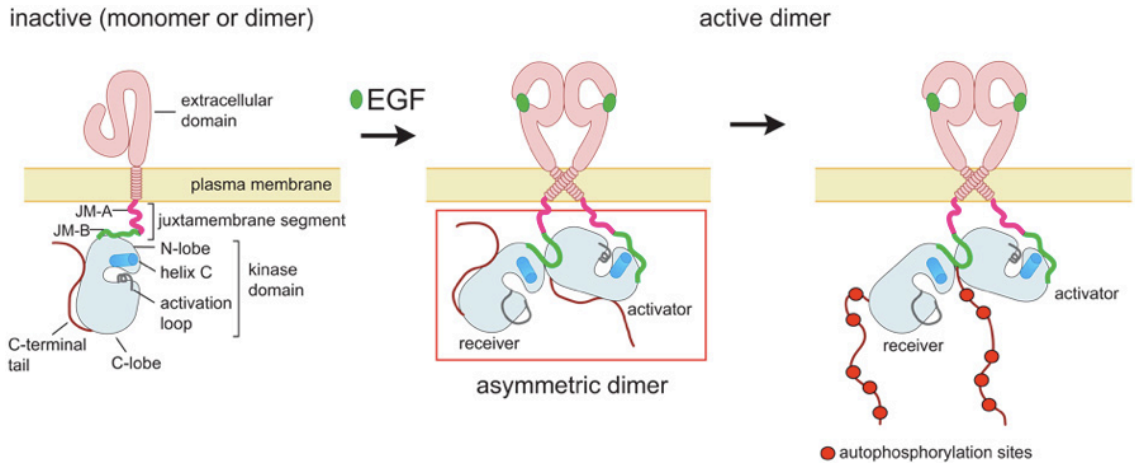

Figure 7. Activation of the intrinsic protein kinase domain. The juxtamembrane region (JM-A and JM-B) is involved in the formation of an asymmetric kinase dimer upon binding of the EGF ligand, forming an activator and a receiver domain (Jura et al. 2009 [43]).

Activation of the kinase domain results in phosphorylation of various tyrosine residues of the regulatory region, releasing activation of numerous downstream signaling pathways. EGFR thereby constitutes a central node in a complex signaling network and coordinates the assembly of different multiprotein complexes, for example by providing a docking site for the scaffold protein Shc. Activated pathways are highly complex and interrelated and include MAPK (Mitogen Activated Protein Kinase), AKT, PLC-γ/PKC (Phospho Lipase C-γ/Protein Kinase C) and JAK/STAT (Janus Kinase/Signal Transducer and Activator of Transcription) pathways [44-46]. This complex network includes numerous positive and negative feedback loops that have significant influence on the time and intensity of the signal. The possible outcomes include affects on proliferation, survival, apoptosis, motility, protein synthesis, and cytoskeletal regulation in somatic cells, tumor invasion and metastasis in tumorigenic cells, and neuronal migration and synapse plasticity in neuronal cells [30]. Figure 8 demonstrates the complex interplay of factors participating in EGFR signal transduction.

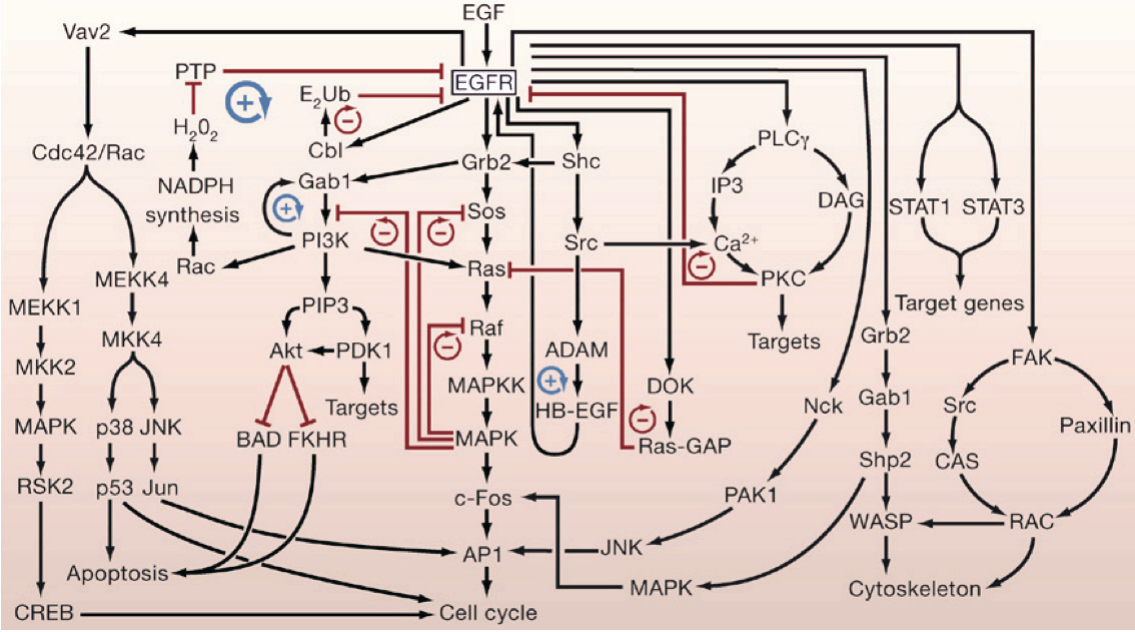

Figure 8. Excerpt of signal pathways activated by EGFR. Red lines depict inhibitory, black lines stimulatory signal mechanisms. Red and blue circles indicate negative and positive feedback loops (Lemmon and Schlessinger, 2010 [30]).

Phosphorylation of the regulatory region leads to rapid internalization of the receptor [47], a mechanism mainly mediated by clathrin coated pits [48]. Endocytosed receptors are then delivered to early endosomes which gradually mature to late endosomes and multivesicular bodies (Figure 9) [49]. Receptors stay activated until the decreasing pH in endosomes causes ligands to dissociate from the receptor. TGFα dissociates rapidly, thereby deactivating the receptor's internal tyrosine kinase domain and making it prone for recycling. EGF on the other hand stays associated with the receptor, leading to its degradation. This mechanism implies that binding of different ligands leads to different signal strengths and time frames and can thereby lead to different stimulatory.

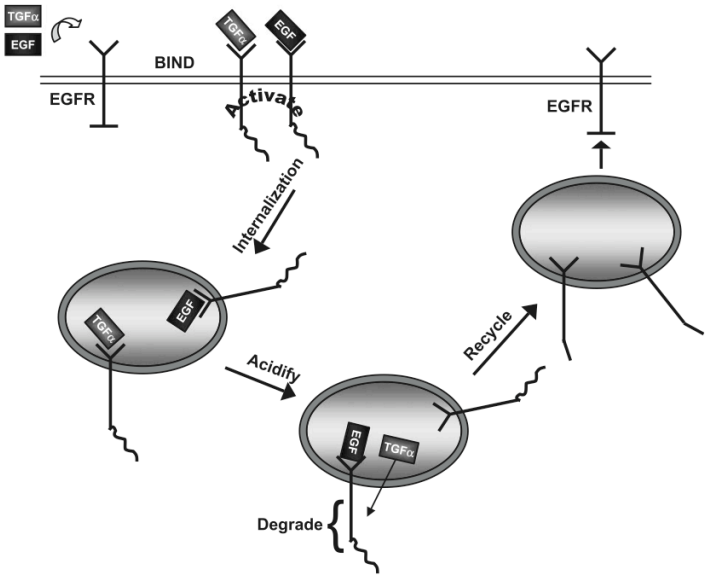

Figure 9. The EGFR "life cycle" [49]. Ligand-receptor complexes are rapidly internalized. Depending on the ligand type, receptors can either become degraded or recycled.

2.4 Juxtacrine Cell Signaling

The term "juxtacrine" was first used by Anklesaria et al. to describe binding of the membrane anchored TGFα ligand to the EGF receptor which led to both cell-cell adhesion and activation of the receptor [27]. Although there is increased evidence that juxtacrine signaling triggers different biological responses when compared to the tightly related autocrine/paracrine signaling, few studies differentiate between those two signaling modes. Nevertheless it has been shown that signaling mediated by a membrane tethered mutant heparin bound (HB)-EGF has different effects on growth, differentiation, migration, motility, branching and adhesion [50, 51]. Other studies indicate a difference in cell growth, migration and adhesion when TGFα was co-expressed with the tetraspanin CD9 which associates with the uncleaved proTGFα and stabilizes it on the cell surface [6, 52]. The same studies suggest a higher level of EGFR activation when TGFα binds to the receptor in a juxtacrine fashion preventing endocytosis of the ligand/receptor complex. This presumably leads to a prolonged and increased signal compared to activation by soluble ligands. In a particularly remarkable finding, MDCK (Madin-Darby Canine Kidney) cells transfected with EGFR and TGFα showed increased DNA synthesis and proliferation while MDCK additionally transfected with CD9 exhibited a growth and proliferation decrease. These phenotypic differences occurred despite transmembrane TGFα and activated EGFR levels that were considerably higher in the CD9 transfected cells. Similarly, in a growth assay with 32D-EGFR cells stimulated with different concentrations of TGFα I could mimic this effect by supplementing the medium with 10 ng/ml recombinant TGFα (see chapter 4.1), which stands in contrast to previous studies [6, 52]. It was found that growth inhibition induced by high EGFR activation levels due to juxtacrine TGFα signaling was accompanied by a significantly

higher expression level of p21CIP1, a potent inhibitor of the cyclin dependent kinase complexes cyclin E/cdk2 and cyclin D/cdk4 [6]. High p21CIP1 levels usually lead to growth arrest [53].

A possible biological function of juxtacrine signaling was proposed by Singh and Harris in which growth of epithelial monolayers of cells expressing EGFR and a membrane anchored ligand is inhibited by high levels of EGFR signaling due to juxtacrine ligand-receptor binding [49]. This inhibition is thought to help maintain the integrity of the monolayer (Figure 10 A). Injury of the monolayer activates metalloproteinases which leads to cleavage of membrane bound growth factors (Figure 10 B). Recently it was shown that Cα cells exposed to different kinds of stress activate p38 MAP kinase which interacts with the cytoplasmic region of TACE, thereby inducing ectodomain shedding of TGFα [23]. Paracrine and autocrine activation of EGFR by soluble ligands then induces cell proliferation and migration into the injured area (Figure 10 C). When the cell monolayer is reconstituted, transmembrane ligand-receptor interactions are again utilized to maintain the integrity of the monolayer (Figure 10 D).

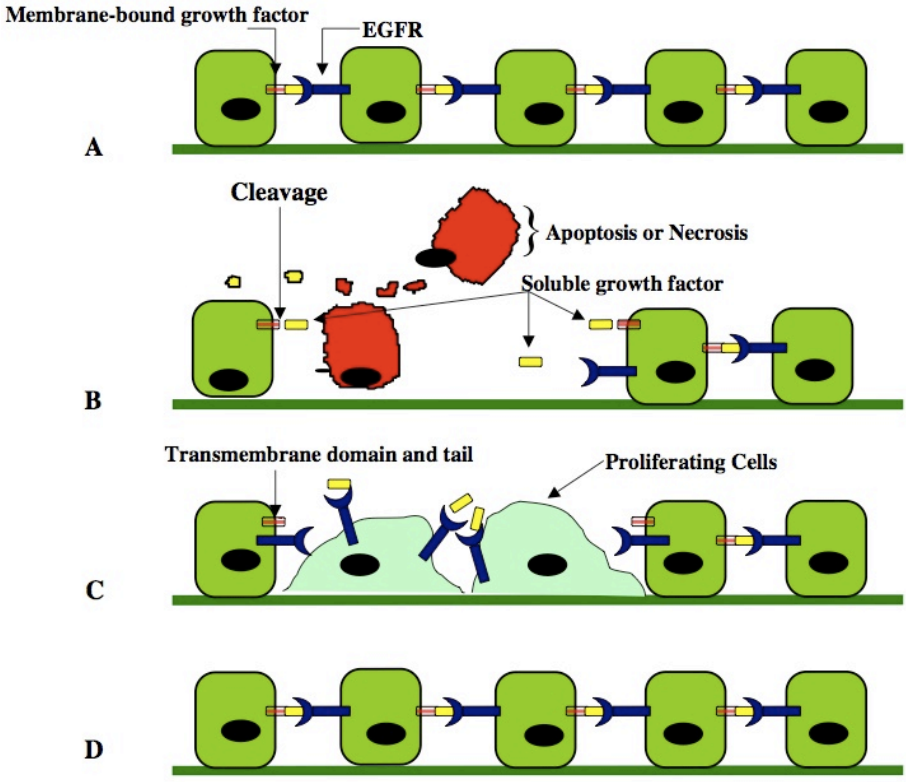

Figure 10. An hypothetical model aiming to explain the biological function of juxtacrine EGFR signaling as proposed by Singh and Harris [49].

3 Experimental Procedures

3.1 Cell Lines and General Cell Culturing

The hematopoietic, interleukin-3 (IL-3) dependent, mouse 32D cell line was transduced using a retroviral vector based on the pBABE puro plasmid containing the human EGFR coding sequence or with control virus lacking the insert. Chinese hamster ovary (CHO) cells were engineered to express the cell surface TGFα ligand. They were similarly transduced with retrovirus constructed from the pBABE puro expression plasmid containing the TGFα coding sequence, or with the empty vector alone.

Cα, a CHO derivative cell line stably expressing TGFα at high levels (kindly provided by the Derynck lab) was used as a positive control for TGFα-infected CHO cells to evaluate TGFα expression levels.

M2 cells are a CHO cell line expressing a mutated form of TACE incapable of cleaving proTGFα (also kindly provided by the Derynck lab). This cell line was used to control for differences between juxtacrine signaling alone and total signaling resulting from a combination of both juxtacrine and paracrine signaling.

The human epidermoid carcinoma cell line A-431 expresses high levels of EGFR and various other EGFR ligands and was used as a positive control for EGFR expression and activated EGFR levels.

WEHI-3 cells were used to prepare IL-3 containing conditioned medium to supplement the 32D growth medium.

All cell lines were cultured with the indicated medium supplemented with 10% FBS (JRC), 100 U/ml penicillin and 100 µg/ml streptomycin in 5% CO_2, water-saturated atmosphere at 37° unless otherwise specified. CHO, Cα, and M2 cells, were grown in F-12 medium. The CHO derivative CHO-TGFα and CHO-pB cells were additionally supplied with 10 µg/ml puromycin to maintain TGFα expression. Cα cells were supplemented with 200 µg/ml geneticin [54]. Cells were passaged every three days at a 1:10 ratio. CHO derivative cells were washed with D-PBS, lifted with 0.25% trypsin for 10 min, and the trypsin neutralized by the addition of full growth medium. The A-431 cell line was cultured in Dulbecco's Modified Eagle's Medium (DMEM). Subculturing was performed by lifting cells with 0.05% trypsin for 10-15 min and split at a 1:8 ratio. The interleukin-3 (IL-3) dependent 32D cell line was cultured in RPMI 1640 medium adjusted to obtain 2 mM L-glutamine, 1.5 g/L sodium bicarbonate, 4.5 g/L glucose, 10 mM HEPES buffer, and 1 mM sodium pyruvate, and 10% previously prepared WEHI-3 conditioned media was added (as described below). To maintain EGFR expression 32D-EGFR cells, as well as 32D-pB cells, were additionally supplemented with 2.5 µg/ml puromycin.

Subculturing was performed by addition of new media at a ratio of 1:10. Cell density was maintained between $2x10^5$ and 10^6/ml.

To prepare WEHI-3 conditioned medium, $5x10^6$ cells were thawed and resuspended in 20 ml full growth medium (Isocove's Modified Dulbecco's Medium). When cells reached a density of $2x10^6$/ml, they were transferred into two large (175 cm^2) flasks and 90 ml full growth media was added to each. After 48h cells were spun down and the supernatant filtered with a 0.22 µm nitrocellulose filter. The conditioned medium was then stored at 4°C until use.

Cryopreservation of cells was generally performed by resuspending cells at a concentration of $5x10^6$/ml in full growth media supplemented with 10% DMSO and aliquoted at 1 ml into cryovials. The cells were frozen at -80°C in a freezing container filled with isopropanol to obtain a constant temperature decrease of -1°C/min. The next day, cells were transferred into liquid nitrogen. Cells were quickly thawed in a 37°C water bath, transferred to 10 ml prewarmed full growth medium, spun down in a conical 15 ml Falcon tube to remove the DMSO from the freezing media, and resuspended in 10 ml full growth medium.

3.2 Generation of Cell Lines Stably Expressing TGFα or EGFR

The 5169 bp pBABE retroviral expression vector containing a puromycin resistance gene (pBABE puro, Addgene plasmid 1764, Bob Weinberg, principal investigator) was used to generate cell lines that stably express either human TGFα or human EGFR [55]. High titer retroviral particles can be easily generated by co-transfection of the pBABE plasmid together with a vector containing *gag*/*pol* (group antigens and reverse transcriptase) sequences and a vector encoding the envelope protein (*Env*). The TGFα and EGFR sequences were kindly provided by the Rik Derynck research group. Both genes were provided inserted in the pRK5 expression vector.

The pBABE vector contains (in the following order) the 5'-LTR (long terminal repeat) containing a promoter, followed by the Psi packaging signal, the multiple cloning site (MCS), the puromycin resistance gene preceded by a SV40 promoter and the 3'-LTR (see Figure 11). The removal of the *gag*/*pol* and the *env* genes between the 5'- and 3'-LTR and incorporation to different plasmids makes the generated virus particles incapable of reproduction and safer in handling. The vector also contains a bacterial origin of replication and an ampicillin resistance gene for selection of transformed bacteria.

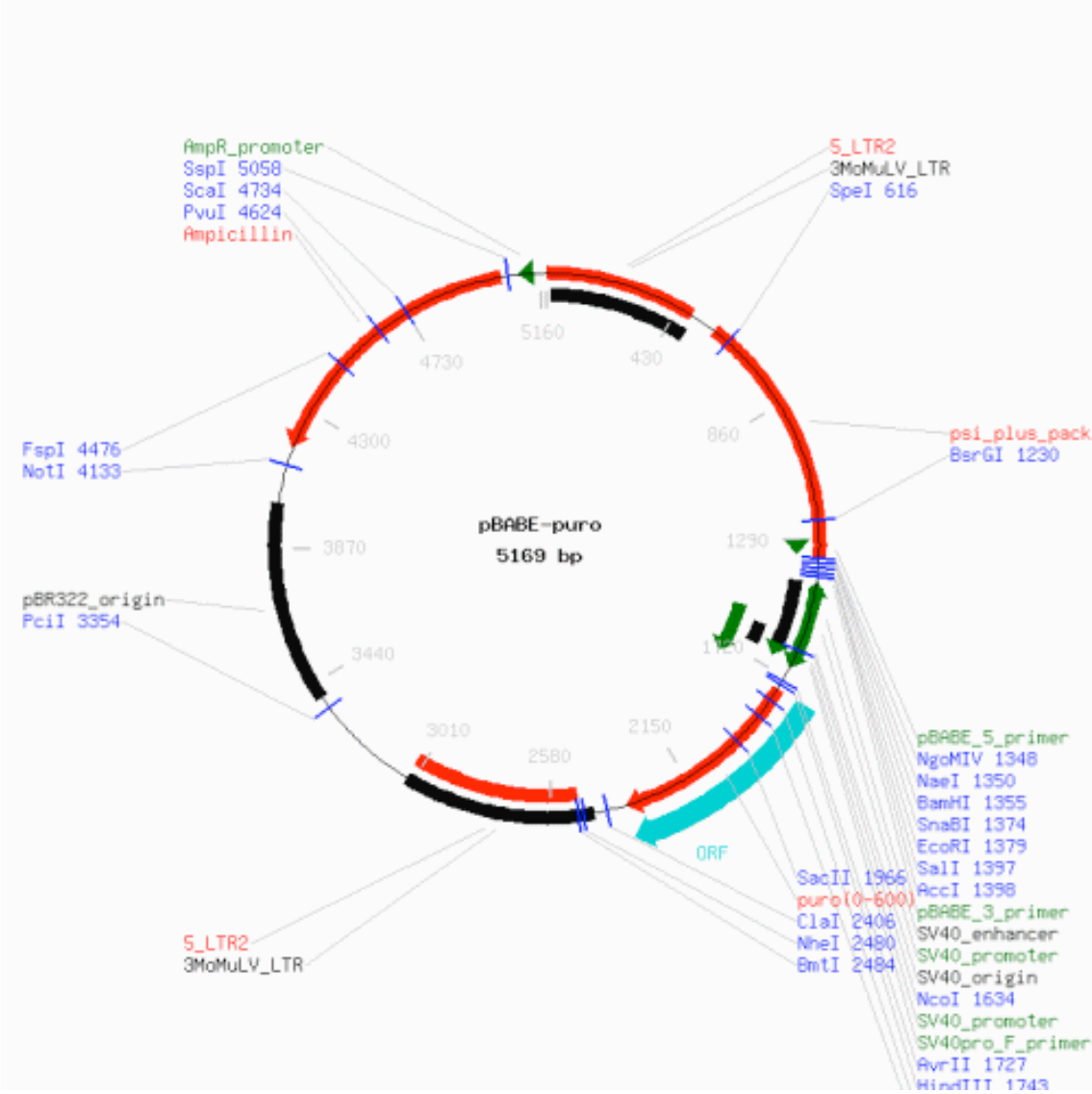

Figure 11. Map of the pBABE puro vector.

To clone the TGFα sequence into the pBABE vector, the pRK5-TGFα plasmid was sequenced and the TGFα coding sequence identified. Forward and reverse PCR primers were designed to amplify the complete coding sequence. Both primer sequences are located outside of the 480 bp coding sequence. The SnaBI restriction enzyme recognition site was added to the 3-prime end of the forward primer, the EcoRI recognition site to the 3-prime end of the reverse primer. Additionally five randomly chosen nucleotides were added to the 3-prime end of each primer to facilitate restriction enzyme digestion of the PCR product. The sequence for the forward primer is 3'-catctaTACGTActgcacctcggttctaagcttatc-5', and the sequence for the reverse primer is 3'-catctaGAATTCttattgatctgccacagtccacctg-5'. Nucleotides depicted in capital letters are the respective restriction sites. PCR was performed with the Phusion High-Fidelity DNA polymerase (Finnzymes) according to the provided manual. The PCR product was loaded on an agarose gel and the DNA band with the predicted size of 618 bp was excised and purified using the QIAquick Gel Extraction Kit (Quiagen). The pBABE puro vector and the PCR product were

double-digested with EcoRI-HF and SnaBI enzymes (New England Biolabs) using buffer NEB 4 and then desalted (QIAquick PCR Purification Kit, Qiagen). Vector and PCR product were ligated at a molar ratio of 1:3 (vector:insert) with T4 DNA ligase (New England Biolabs). DH5α *E. coli* were transformed with the ligation product, plated on LB-agarose containing 100 µg/ml ampicillin, and incubated overnight. A total of 26 clones were picked and selectively grown in LB broth containing ampicillin for 8 hours. The plasmids were isolated using the QIAprep Spin Miniprep Kit (Qiagen) and a sample was digested with HindIII and loaded onto an agarose gel to perform an analytical digest. One HindIII restriction site is located on the pBABE puro vector, and another within the TGFα sequence. Thirteen clones containing the insert were identified. Sequencing of the cloned plasmids confirmed the correct incorporation and lack of any DNA polymerase errors. Two clones were amplified for future use.

The same procedure was applied to insert the EGFR sequence into the pBABE puro vector, with the following modifications: due to the existence of EcoRI restriction sites within the EGFR sequence, the reverse primer was extended with a SalI recognition site instead. The forward primer sequences is 5'-atataTACGTAgagcttatcgattctagccgagtc-3' and is located on the pRK5 vector. The reverse primer sequence is 5'-atataGTCGACgctcatactatcctccgtggtcat-3' and is located on the mRNA sequence preceded by the 3630 bp coding sequence. Eleven clones were picked. The analytical digest of the cloned plasmid was carried out using SnaBI and SalI and four clones containing the EGFR insert could be identified. For sequencing of the 3774 bp inserted region a set of five successive primers spaced roughly 800 bp apart was used.

To test the function of the pBABE-puro-TGFα and the pBABE-puro-EGFR plasmids, CHO or 32D cells respectively were transfected using the Lipofectamin 2000 reagent (Invitrogen) and the TransIT 2020 reagent (Mirus). TGFα could be detected in CHO cells using either of the two reagents but EGFR expression of 32D cells could not be confirmed. The test was carried out by standard Western Blotting using the primary antibodies GF06 Anti-TGF-α Ab-1 (134A-2B3) (Calbiochem) and the EGFR (EGF-R2) sc-73511 (Santa Cruz Biotechnology), an HRP-conjugated (horseradish peroxidase) secondary antibody and an ECL kit (GE Healthcare). Transfection of 32D cells with a vector containing the GFP gene as positive control did not result in any fluorescence, suggesting very low transfection efficiency of 32D cells. However, EGFR could be detected by transfecting CHO cells, confirming proper function of the plasmid.

To generate infectious retrovirus particles, HEK 293 cells were co-transfected with (1) the pBABE plasmid containing either EGFR, TGFα or the vector without any insert, (2) a *gag*/*pol* expression vector, and (3) an *env* expression vector encoding the pantropic VSV-G envelope protein (vesicular stomatitis virus G protein). This system is not dependent on a specific packaging helper cell line. HEK 293 cells were chosen because of the high transfection efficiency using the Mirus TransIT-293 transfection reagent. Forty eight hours after transfection the media was collected, sterile filtered with a 0.45 µm nitrocellulose filter, aliquoted and stored at -80°C.

CHO and 32D cells were infected with virus containing either TGFα or EGFR and the puromycin resistance gene, or with virus containing only the pBABE puromycin resistance gene (pB), leading to a total of four cell lines (CHO-TGFα, CHO-pB, 32D-EGFR, and 32D-pB). CHO cells stably incorporating TGF-alpha were selected for with 10 µg/ml puromycin, while 32D cells expressing EGFR were selected for with 2.5 µg/ml puromycin for four days. Single colonies were selected by diluting to a cell concentration of approximately 2 cells/ml and distributing 100 µl to each well of a 96-well plate. After one week, wells containing colonies were identified, six clones of each of the four cell lines were grown up, and CHO-TGFα and 32D-EGFR clones were tested for their expression level of TGFα or EGFR respectively via Western Blotting. The clone with the highest protein expression was selected and used for future experiments. All clones were grown up to a high density, frozen, and stored in liquid nitrogen using a standard cryopreservation protocol and full growth medium supplemented with 10% DMSO (dimethyl sulfoxide).

The puromycin concentrations used for selection and maintenance were determined by a previous cell growth assay using puromycin concentrations ranging from 1 to 20 µg/ml. Cell viability was measured over a period of six days by adding resazurin to the cells growing in a 96-well plate with transparent flat bottom. Resazurin is metabolized by living cells to resorufin which has a fluorescence peak at 585. Fluorescence was measured four hours after addition of resazurin using a Tecan Safire plate reader. A concentration of 10 µg/ml for CHO cells and a concentration of 2.5 µg/ml for 32D cells was determined to kill all cells not containing the resistance gene after 3 days.

3.3 Cell Lysates, SDS-PAGE and Immunoblotting

Cells were lysed with RIPA buffer (150 mM sodium chloride, 1% NP-40, 0.5% sodium deoxycholate, 0.1% SDS, 50 mM Tris pH 8) supplemented with a protease inhibitor mix (complete Mini EDTA free, Roche), 100 µM Na_3VO_4 (sodium orthovanadate), and 100 µM PMSF (phenylmethanesulfonylfluoride). The total protein concentration was measured with the BioRad DC Protein Assay with a BSA dilution series as standards. An equal amount of 40 µg per sample was denatured with 100 mM DTT (dithiothreitol) and a protein loading buffer (5x containing 0.313 M Tris HCl (pH 6.8), 10% (w/v) SDS, 0.05% (w/v) bromophenol blue, 50% (v/v) glycerol) for 5' at 95°C, loaded onto a BioRad Criterion Tris-HCl 4-20% polyacrylamide gel and run for 1h at 200 V in tris-glycine buffer supplemented with 0.1% SDS. Subsequently the proteins were blotted on a 0.45 µm pore size nitrocellulose membrane for 1.5 hrs at 100 V in tris-glycine buffer containing 10% methanol (20% methanol was used for the transfer of TGFα). Ponceau S staining solution (BioRad) was used to confirm efficient and uniform transfer.

Immunoblotting for TGFα and EGFR was generally performed by first blocking the membrane with 5% (w/v) non-fat dry milk in TBS-T for 1h at room temperature. The blot was incubated with either monoclonal mouse anti TGFα Ab-1 (Calbiochem) at a 1:100 concentration,

or monoclonal mouse anti EGFR (EGF-R2) (Santa Cruz Biotechnologies) at a 1:500 concentration overnight at 4°C in 5% milk-TBS-T. The anti TGFα antibody binds to the mature soluble part of TGFα. The anti EGFR antibody binds EGFR at the extracellular region. Incubation with a horseradish peroxidase conjugated anti mouse IgG secondary antibody (Abcam) was performed for 1 hr at room temperature in 5% milk-TBS-T. The Amersham Hyperfilm and ECL detection reagents (GE Healthcare) were used to develop the blots.

The Licor Odyssey Infrared Imaging System was used for quantitative immunoblotting. The membrane was first blocked with Odyssey Blocking Buffer (without Tween 20) for one hour at room temperature. The membrane was then incubated with monoclonal rabbit anti phospho-EGFR at Tyr1068 (Cell Signaling, #2234) and mouse monoclonal anti α-tubulin (Calbiochem, CP06), both at a concentration of 1:1000 in TBS-T (tris-buffered saline with 0,1% Tween 20) supplemented with 5% (w/v) BSA (bovine serum albumin) overnight at 4°C. As secondary antibodies, IRDye 800CW Goat Anti-Rabbit and IRDye 680LT Goat Anti-Mouse (Licor) were used at a 1:10000 concentration in Odyssey Blocking Buffer supplemented with 0.1% Tween 20. The blot was incubated at room temperature for one hour, washed three times with TBS-T and one time with Milli-Q water to remove residual Tween 20 which otherwise would increase background fluorescence. The blot was then scanned with the Odyssey Imager and the results evaluated.

In order to determine levels of TGFα shedding, conditioned media of A-431 cells, the infected CHO population heterogeneously expressing TGFα (the population used for the production of single clones), Cα cells, M2 cells, and CHO cells infected with the pBABE vector without insert (CHO-pB) as a negative control was prepared. This was achieved by growing the cell lines in 10 cm petri dishes to 90% confluency and subsequent incubation with serum-free medium for 24 hours. Ten ml of each conditioned medium were then sterile filtered and concentrated to approximately 300 µl using Amicon Ultra centrifugal filter units (Millipore) with a molecular weight cut-off of 3 kDa and 20 µl were loaded onto the protein gel and the blot was incubated with the anti TGFα antibody.

3.4 EGFR Activation and Growth Stimulation Assays

EGFR activation kinetics were determined by stimulating $1x10^6$ 32D-EGFR cells for each time point with 20 ng/ml commercial TGFα protein (purchased from Abcam) in a 12-well plate. Subsequent Western blotting was performed as described above.

Different TGFα concentrations were tested for their effect on EGFR activation. Commercial TGFα protein or Cα conditioned medium were used for stimulation of 32D-EGFR cells at indicated concentrations. Conditioned medium was prepared by incubating Cα cells in a 10 cm petri dish (grown to 80% confluency) with full growth medium. After 12h the medium was sterile filtered (0.22 µm) and used for the assay at indicated dilutions (chapter 4.2).

Growth assays were carried out by treatment of 32D-EGFR cells with different concentrations of recombinant TGFα protein. The assay was performed by seeding 250 32D cells in a volume of 100 µl into wells of a 96-well plate. Every condition and time point was evaluated in triplicate. Live cell numbers were evaluated by adding 10 µl resazurin to the wells and measuring the fluorescence with a plate reader (Tecan Safire).

Activation assays in co-culture conditions were performed by adding TGFα expressing cells at varying cell numbers with $1x10^6$ 32D-EGFR cells in prewarmed 10 ml assay medium (1:1 mixture of PBS and 32D full growth medium) in conical 15 ml Falcon tubes. Samples were first pelleted by centrifugation at 750 g for 3 min and then incubated in a 37°C water bath. Samples not pelleted were put on a spinning wheel in a 37°C incubator. After incubation, all samples were put on ice immediately, cooled to 0°C, centrifuged at 900 g (4°C), lysed, and either stored at -80°C or immediately analyzed by Western blotting.

3.5 Functionalizing Cell Surfaces with DNA-Oligonucleotides

Two 20 bp sequences of DNA (either $(CAGT)_5$ or $(ACTG)_5$) were synthesized on an PE Biosystems Expedite 8905 nucleic acid synthesizer and modified with a 5'-C_6 S-S thiol modifier (1-O-Dimethoxytrityl-hexyl-disulfide,1'-[(2-cyanoethyl)-(*N*,*N*-diisopropyl)]-phosphoramidite, Glen Research). The oligonucleotides were HPLC purified and lyophylized with a Labconco lyophylizer. Disulfide DNA was reduced with tris(2-carboxyethyl)phosphine (TCEP) to obtain 5'-thiol-C_6 single stranded DNA (ssDNA). The oligonucleotides were reconstituted in deionized H_2O at a concentration of 5 mg/ml, aliquoted (50 µl each), and stored at -20°C until used. Succinimidyl-[(*N*-maleimidopropionamido)-hexaethyleneglycol] ester (NHS-PEG_6-maleimide), purchased from Sigma-Aldrich, was reconstituted in anhydrous dimethyl sulfoxide (DMSO) at a concentration of 5 mg/ml, aliquoted (20µl each), and stored at -20°C as well.

Prior to cell surface labeling, 50 µl aliquots of the 5'-thiol-C_6-ssDNA were desalted with an H_2O-pre-equilibrated size exclusion column (Centri Spin 10, Princeton Separations) and reacted with 20 µl aliquots of NHS-PEG_6-maleimide for 10 min at room temperature to obtain NHS-modified ssDNA. The reaction solution was passed through a second size exclusion column pre-equilibrated with PBS (phosphate buffered saline) solution (pH 7.2). The flow-through of all columns was mixed together and 50 µl per 10^6 cells were used for subsequent DNA-labeling.

For the treatment of cell surfaces with NHS-DNA, CHO derivative cells were first lifted with 0.4% EDTA (ethylenediaminetetraacetic acid) in D-PBS (PBS without Ca^{2+} and Mg^{2+}). To prevent cleavage of surface proteins, trypsin was generally avoided where possible. If necessary, a quick trypsin pulse with 0.05% trypsin was applied (45-60 seconds) and subsequently quenched with soybean trypsin inhibitor. 32D and CHO cells were then washed

three times in D-PBS and incubated for 30 min with freshly prepared NHS-DNA (50 µl per 10^6 cells). The use of Ca^{2+} and Mg^{2+} free PBS prevents cells from reattaching to surfaces or non-specifically aggregating. After treatment, cells were washed three times with PBS supplemented with 1% FBS (fetal bovine serum).

To quantify the number of DNA-oligonucleotides attached to the cell surfaces, a portion of the labeled cells were incubated with a 6-FAM (6-carboxyfluorescein) conjugated complementary DNA probe for 30 min on ice. After washing three times in PBS plus 1% FBS, cells were analyzed on a flow cytometer (FACScalibur, BD Biosciences) together with beads containing a defined number of fluorescein molecules (Quantum FITC-5 MESF, Bangs Biolabs Inc.). The quantitation kit contains six kinds of beads, including five with different FITC (fluoresceinisothiocyanate) fluorescence intensities, and one blank. A standard curve can be drawn in order to identify the respective MESF units (Molecules of Equivalent Soluble Fluorochrome) of the samples.

The efficiency of cell assembly was also measured by flow cytometry. CHO cells were stained with CellTrace Far Red DDAO-SE (Invitrogen) and 32D cells with CellTracker Green CMFDA (Invitrogen). After labeling cells with complimentary DNA strands as described above, CHO and 32D cells were mixed together at a ratio of 1:100 (CHO:32D) in a 24-well low attachment plate (Corning) for 15 min at room temperature with gentle agitation at a density of 10^6 cells/ml. As cells tend to form clumps at lower ratios, the ratio was maintained above 1:50 to avoid clogging of the flow cytometer. Assembled populations were then loaded onto the flow cytometer for analysis. Events were plotted as a scatter plot using fluorescence values recorded on the FL1 (green) and FL4 (infrared) channels.

4 Results and Discussion

4.1 Recombinant Protein Expression Levels and TGFα Shedding

In order to confirm the function of the pBABE puro plasmid with TGFα or EGFR inserted into the multiple cloning site, CHO cells were transiently transfected with pBABE using the Lipofectamine 2000 (Invitrogen) reagent. Due to very low transfection efficiency (as determined by previous experiments), the function of the plasmid could not be confirmed by transfecting 32D cells. Figure 12 shows the anti EGFR immunoblot. CHO cells were transfected with the pBABE vector only (CHOpB) and with the vector containing the EGFR gene, and cell lysates were prepared 24h and 42h post transfection. A-468 and A-431 cell lysates were loaded as positive controls onto the gel. A-431 epidermoid carcinoma cells have previously been shown to express EGFR and TGFα at high levels [56].

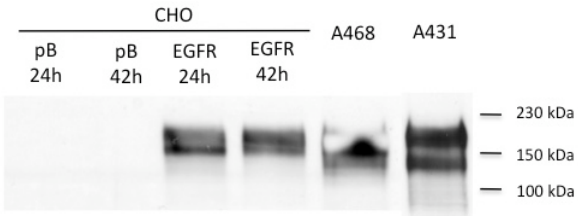

Figure 12. Immunoblot of CHO cells transiently transfected with vector only (pB) or with EGFR and cultured for 24h and 42h. A468 and A431 cell lysates are included as a positive control.

The same procedure was performed for the pBABE-TGFα plasmid. Figure 13 shows that transiently transfected CHO cells express TGFα only at a low level compared to Cα cells. CHO-pB and CHO cells without any vector were used as negative controls.

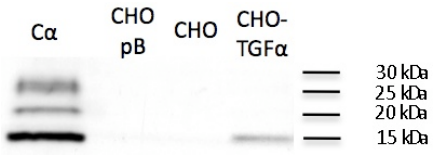

Figure 13. Transiently transfected CHO cells express a 15 kDa transmembrane TGFα species.

Generation of retrovirus, infection and production of single clones was accomplished as described above (chapter 3.2). TGFα expression was evaluated by Western blotting. Figure 14 shows relative levels of TGFα expression for five clones. To determine levels of TGFα shedding, 24-hour conditioned media of A-431 cells, of the infected CHO population heterogeneously expressing TGFα (the population used for the production of single clones), of Cα cells, of M2 cells, and of CHO cells infected with the pBABE vector without insert was also loaded onto a denaturing PAGE gel. Cα cell lysates and 10 ng of recombinant TGFα protein were used as controls.

Figure 14 illustrates that the CHO-TGFα clones express TGFα at different levels. The band is located at about 15 kDa, consistent with a species incorporating the transmembrane domain but with the prodomain proteolytically removed [23]. Two higher molecular weight bands are barely visible in the CHO-TGFα cells but are prominent in the Cα cell lysate. These bands are located at about 20 and 25 kDa. The lower molecular weight band presumably corresponds to the precursor protein with the N-terminal unglycosylated prodomain. This species is likely primarily located in the endoplasmatic reticulum [23]. The higher molecular weight band belongs to the same precursor but incorporating an N-glycosylated proregion predominantly located in the golgi. Clone six showed the highest expression level and was therefore selected for future experiments.

Conditioned media of A-431 cells and the heterogeneous population of TGFα-expressing CHO cells did not contain detectable amounts of soluble TGFα which might be due to either a low level of TGFα shedding or to a generally low expression level. Unexpectedly, TGFα could not be detected in A-431 cell lysates either (data not shown). The 5 kDa band in the Cα conditioned media corresponds to the soluble mature TGFα protein, which runs at a similar molecular weight compared with the recombinant protein at the right side of the blot. The more diffuse band between 18 and 20 kDa belongs to two different N-glycosylated soluble TGFα species containing the uncleaved proregion [13].

As expected, CHO-pB and M2 cells do not secret TGFα into the media. M2 stably express HA-tagged rat TGFα [57] which is detected by the same antibody. The bottom band very likely corresponds to the bottom band seen in CHO-TGFα and Cα lysates. Three additional TGFα species can be seen which have different sizes than the species seen in CHO-TGFα or Cα. This might be due to a different processing of rat TGFα compared to the human protein.

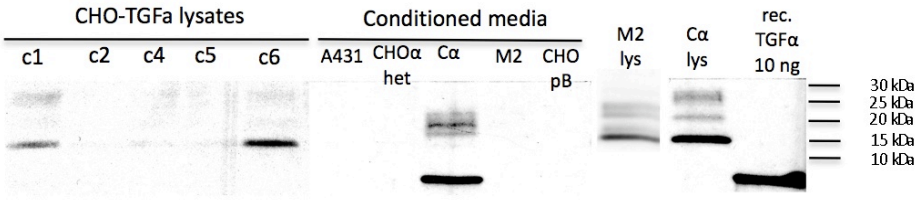

Figure 14. TGFα expression of clones of infected CHO cells and soluble TGFα in conditioned media of various cell types. M2 and Cα lysates as well as 10 ng recombinant TGFα were also included.

4.2 EGFR Activation Kinetics in 32D-EGFR cells

To maximize the signal level of activated EGFR for detection by quantitative Western blotting, knowledge about activation kinetics is crucial. Activation of EGFR in 32D-EGFR cells was measured by the phosphorylation level of Tyr 1068 which provides a binding site for the adaptor protein Grb2, resulting in activation of MAPK/Erk signaling, and Gab1, leading to activation of the AKT/PKB cascade.

In brief, 32D-EGFR cells were stimulated with 20 ng/ml TGFα for different time periods and 40 µg of whole cell lysates was analyzed by quantitative Western blotting. Figure 15 shows the integrated fluorescence intensities of the immunoblot analyzed with the Licor Odyssey system. After addition of TGFα to the medium, activation level increases rapidly and reaches a maximum after 20 minutes. Maximum activation is presumably achieved between 15 and 30 minutes. The maximum peak is followed by a gradual decrease due to receptor and ligand internalization.

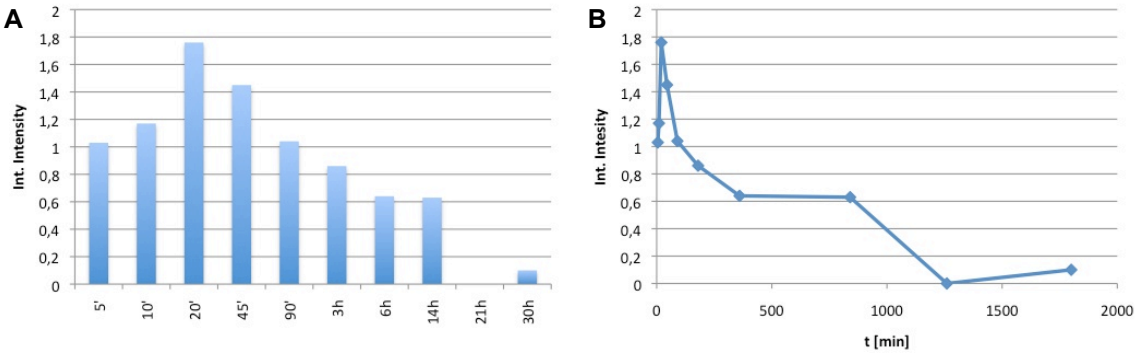

Figure 15. EGFR activation levels at times indicated. The integrated fluorescence intensities of the phosphorylated EGFR bands of the immunoblot are depicted as histogram (A) and as an xy-plot over time (B). Points in (B) were connected to better visualize the progression over timer.

In another experiment, 32D-EGFR cells were co-cultured with CHO-TGFα cells and lysates were prepared at different time points. Stimulation was performed by adding $2x10^5$ CHO-TGFα cells to $1x10^6$ 32D-EGFR cells (1:5 ratio) in 10 ml of assay medium (see chapter 3.4). The resulting cell suspensions were either pelleted to simulate cell assembly or maintained in suspension prior to incubation. A maximum level of EGFR phosphorylation could be detected after about 1 hour (data not shown). The slower kinetics of EGFR activation by co-culturing are presumably due to the fact that at time point 0 no TGFα exists in the medium. Only after a certain period of time would TGFα expressing cells have secreted enough soluble TGFα to cause detectable amounts of activated EGFR. In contrast, 32D-EGFR cells exposed to conditioned media immediately experience stimulation by soluble TGFα..

To ensure EGFR activation was minimal during prolonged incubation at 4 ˚C (as would be required during DNA-templated cell assembly), receptor phosphorylation at 4°C was compared to 37°C. One million 32D-EGFR cells were incubated with 20 ng/ml TGFa for 30 minutes and activation levels monitored by quantitative Western blotting. Figure 16 illustrates that the difference of activation at 37° is about 10-fold higher than at 4°C. This difference in activation levels is sufficient for future assembly/activation experiments.

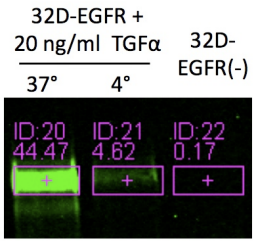

Figure 16. Activation of 32D-EGFR cells by stimulation with 20 ng/ml TGFa for 30 minutes at either 37°C or 4°C.

4.1 32D-EGFR TGFα Growth Stimulation

The hematopoietic myeloid cell line 32D is absolutely dependent on IL-3 for its proliferation and survival. Although EGFR is not expressed in 32D cells, all necessary downstream components to produce a mitogenic response stimulated by this factor are available. This was demonstrated by propagation of 32D cells transfected with EGFR in the absence of IL-3 but in presence of EGF [27, 58]. I undertook different growth assays to confirm the proper function of the EGFR construct and the possibility of stimulating a mitogenic signal in retrovirally infected 32D-EGFR cells.

On day 0, 250 32D-EGFR cells were seeded in triplicate into 96-well plates in full growth medium (containing IL-3) in the presence of different concentrations of recombinant soluble TGFα. Cell numbers were determined by addition of resazurin and measuring the resulting fluorescence using a plate reader after four hours. Figure 17 shows a significant growth advantage within the first four (out of six) days even in the presence of a remarkably low TGFα concentration (0.01 ng/ml, corresponding to 1.8 pM assuming a molecular weight of 5552 g/mol). A growth assay with 32D cells not containing the pBABE-EGFR plasmid was also performed as a negative control and resulted in no growth stimulatory effect of TGFα (Figure 18).

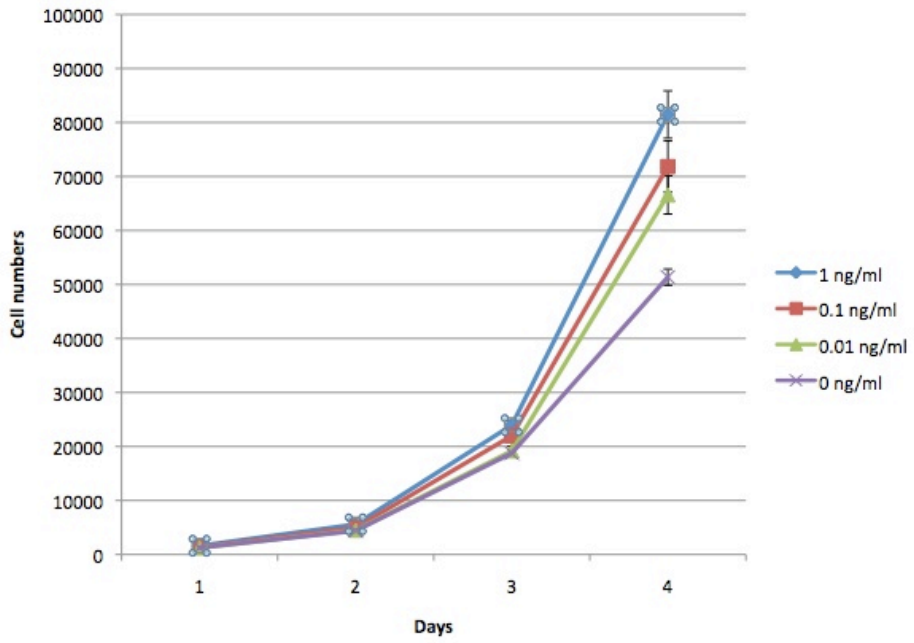

Figure 17. Four-day growth assay of 32D-EGFR cells incubated in full growth medium (containing IL-3) supplemented with different amounts of TGFα as indicated in the legend.

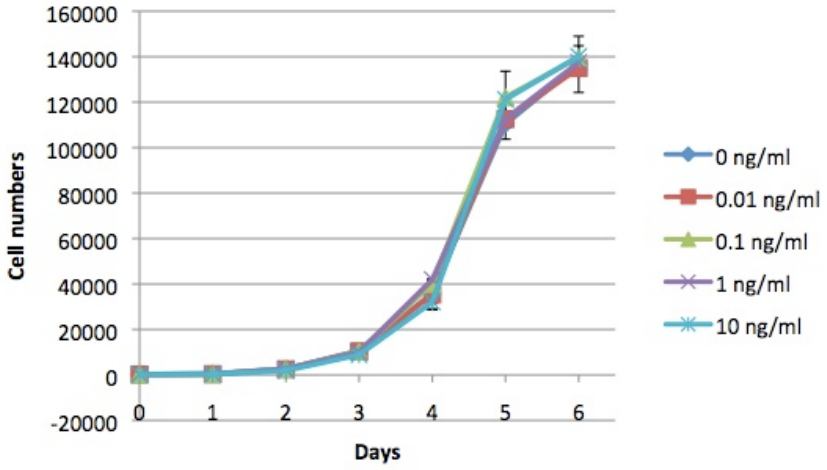

Figure 18. Growth of 32D cells not expressing the EGF receptor. No significant difference can be observed.

Figure 19 shows all six days of the same experiment with three different TGFα concentrations plotted. A moderate amount of TGFα (0.1 ng/ml or 18 pM) leads to a slight growth advantage during the first four to five days compared to the control. A hundred fold higher concentration (10 ng/ml or 1.8 nM) leads to a clear growth arrest after day 4. This behavior could not be verified in previous studies [6, 52], which might be explained by a higher level of EGFR expression in the 32D-EGFR cells used for this experiment.

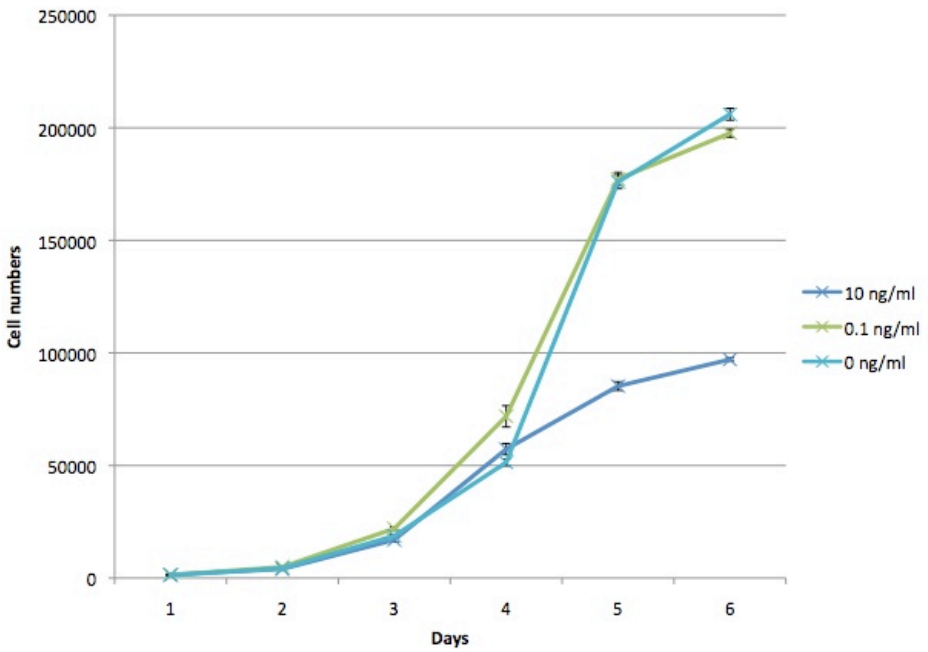

Figure 19. Six-day growth assay of 32D-EGFR cells incubated either without, with a moderate amount, or with a high amount of TGFα to demonstrate the possibility of stimulating growth arrest with a high level of TGFα-EGFR signaling.

The same experimental set up was used to investigate the possibility that 32D-EGFR might survive in the absence of IL-3 if stimulated by TGFα (Figure 20). All concentrations previously found to stimulate growth did not overcome the requirement for IL-3. However, TGFα present at 10 ng/ml allowed cell survival but without significant growth.

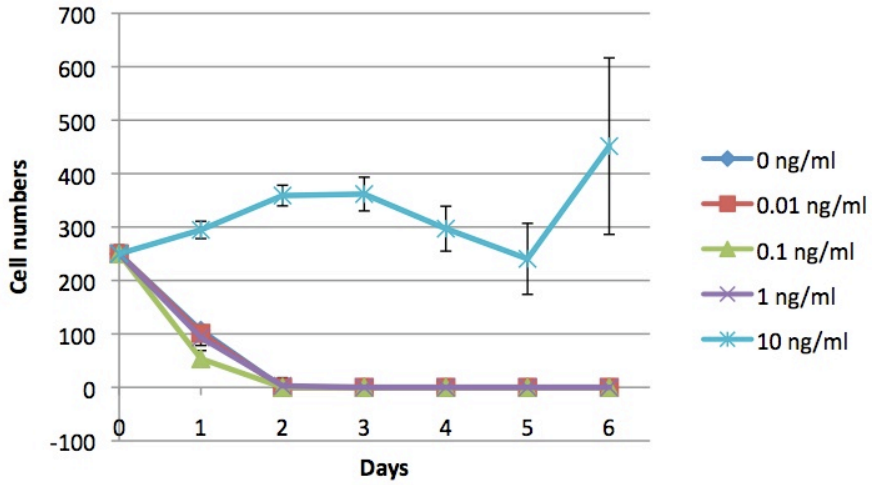

Figure 20. Growth assay demonstrating survival of 32D-EGFR cells stimulated with 10 ng/ml soluble TGFα in the absence of IL-3.

4.2 Selection of an Appropriate TGFα Expressing Cell Line

Three cell types were analyzed for their ability to activate EGFR in 32D-EGFR cells. The aim was to determine conditions resulting in a high juxtacrine-to-paracrine signal ratio and in a generally high level of activation to facilitate the detection of phosphorylated EGFR. As the retrovirally infected CHO-TGFα cell line is expressing TGFα at rather low levels, an initial idea was to use the Cα cell line expressing higher levels of TGFα to increase overall EGFR activation. To obtain a first impression of the level of EGFR activation in 32D-EGFR cells stimulated with TGFα produced by Cα cells, 32D-EGFR cells were stimulated with different concentrations of recombinant TGFα protein and with different dilutions of 12 hrs Cα conditioned medium for two hours (see Figure 21). A-431 cell lysate and lysate of unstimulated 32D-EGFR cells were used as controls.

As expected, EGFR phosphorylation levels increased with higher concentration of TGFα in the medium. Receptor activation could be detected at a TGFα concentration of 1 ng/ml, corresponding to 180 pM (assuming a molar weight of 5552 g/mol). Interestingly, stimulation with different dilutions of Cα conditioned medium did not show significant differences in activation levels, indicating that Cα cells secrete TGFα into the medium at a level which saturates the receptor internalization process as proposed by Wiley et al. [59]. The slight variations in the band intensities might be due to a rather unpredictable behavior of EGFR phosphorylation levels at high ligand concentrations. A-431 cells express a variety of EGFR ligands and activate EGF receptors in an autocrine fashion. Ligand expression combined with a general high EGFR expression levels leads to steadily high activation levels.

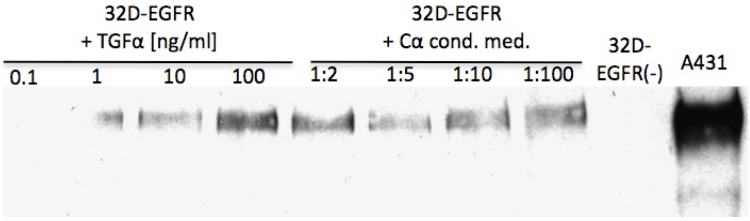

Figure 21. EGFR phosphorylation in stimulated 32D-EGFR cells. Cells were incubated with recombinant TGFα or Cα conditioned medium at indicated concentrations.

The fact that the lowest concentration of Cα conditioned medium (1:100) led to a similar level of activation of the highest concentration (1:2) suggests that EGFR activation was saturated. The maximum number of phosphorylated EGFR is likely determined by a combination of the total number of EGF receptors on the cell surface, the speed of endocytosis, the ratio of internalized receptors undergoing degradation versus receptors being recycled, and the expression of new EGFRs. This finding is in concordance with other studies which suggested that the most important EGFR internalization process via clathrin coated pits has only a limited capacity [59, 60].

Generally, it is plausible that due to the many influencing factors (internalization, degradation/recycling, expression of new EGF receptors, different phosphorylation kinetics of

the various tyrosine residues, etc.) and their different time scales, the level of EGFR activation cannot be easily modeled. At excess levels of ligands, EGFR activation might even behave in a chaotic fashion once the process of increased endocytosis due to phosphorylation and ubiquitination of the receptors cytosolic region is triggered. At excessive TGFα concentrations, a small change of the initial conditions might lead to a very different behavior of the level of activation measured over a certain period of time, until an equilibrium of all factors is reached. Similarly, the different TGFα species present in the conditioned medium could have different affinities to the receptors which affects the time of a receptor dimer staying activated after endocytosis. This could lead to different fates of the receptors (recycling or degradation) which might contribute to a volatile behavior of phosphorylated EGFR levels.

In contrast, EGFR stimulation through addition of lower amounts of TGFα to the medium apparently leads to more predictable kinetics of phosphorylated EGFR levels. In this case the internalization process is not saturated and internalization of receptor-ligand complexes presumably leads to a gradual decrease of TGFα in the medium. This suggests a rapid increase of phosphorylated EGFR after stimulation until a certain maximum level, followed by a gradual decrease. This is consistent with the results in chapter 4.2. However, an additional experiment to determine TGFα levels in the medium over time should be performed. This could be done by quantitative Western blotting with samples of concentrated medium at different time points.

In order to reduce shedding of TGFα and thereby maximizing the contribution of juxtacrine signaling to overall EGFR activation, the TACE inhibitor TAPI-1 (Sigma) was tested for its inhibitory capacity. 32D-EGFR cells were stimulated with a 1:2 and 1:100 dilution of Cα conditioned medium, which was obtained by incubating Cα cells with full growth medium supplemented with different concentrations of TAPI-1. The respective amounts of TAPI-1 were diluted in 25 µl DMSO per 2.5 ml of complete Cα growth medium for $7x10^5$ cells for each TAPI-1 concentration. One cell sample stimulated with conditioned medium of untreated Cα cells and one vehicle control (0 v.c.) only containing DMSO for each of the two conditioned medium dilutions were included. Unstimulated 32D-EGFR cells serves as negative control.

The quantitative Western blot in Figure 22 shows the levels of phosphorylated EGFR for the 1:2 dilution of Cα conditioned medium. High levels of phosphorylated EGFR relative to controls indicates an excessive amount of soluble TGFα in the medium that is not reduced in a dose dependent manner by added TAPI-1. However, a gradual decrease of phosphorylation is observed in lysates of cells treated with the 1:100 dilution of the Cα conditioned medium. Figure 23 shows the same blot after protein transfer stained with Ponceau S solution to confirm equal protein loading and transfer.

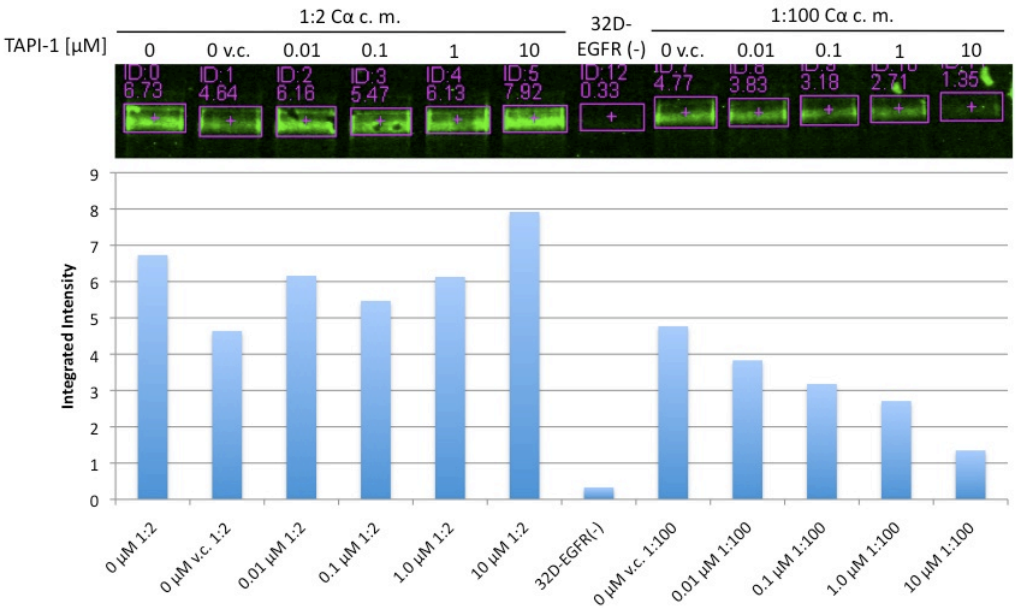

Figure 22. EGFR phosphorylation levels of 32D-EGFR cells stimulated with Cα conditioned medium at different dilutions. Cα conditioned medium was obtained by incubating Cα cells with full growth medium containing different amounts of the TACE inhibitor TAPI-1. The inhibitor was reconstituted in DMSO. One cell sample stimulated with conditioned medium of untreated Cα cells and one vehicle control (0 v.c.) only containing DMSO for each of the two conditioned medium dilutions were included. Unstimulated 32D-EGFR cells serves as negative control.

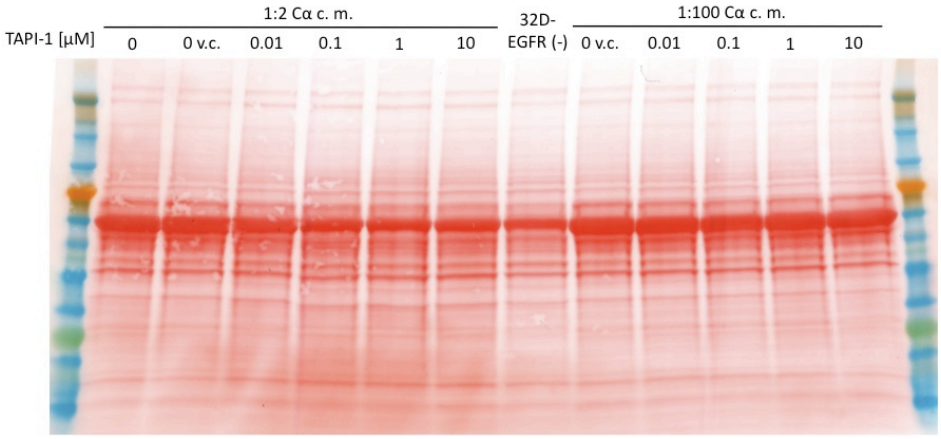

Figure 23. Ponceau S stain of the above immunoblot was used to confirm equal protein loading.

The final aim of the project was to physically attach TGFα expressing cells to EGFR expressing cells, thereby inducing EGFR signaling. Specifically, the aim was to investigate the efficiency of juxtacrine signaling alone without interference by shedded soluble TGFα. This should be possible by subtracting the portion of signaling induced by shedded soluble TGFα from overall EGFR activation in the physically tethered cells. Activation due to shedded TGFα can then be accounted for by incubating EGFR expressing cells with conditioned media of the same cell number of TGFα expressing cells for the same period of time as would be expected for co-culturing. I assumed that the high secretion level of Cα cells would be problematic,

inevitably leading to a saturated level of EGFR activation even in the presence of a high concentration of the TAPI-1 inhibitor. A differentiation between a paracrine and juxtacrine signaling mechanism would then be impossible. The Cα cell line was therefore ruled out as a candidate for subsequent investigations.

After the exclusion of the Cα cell line, CHO-TGFα and M2 cells where analyzed for their ability to stimulate EGFR. For this experiment, 10^6 32D-EGFR cells were incubated for 25 min in 10 ml assay medium with $2x10^5$ of either CHO-TGFα or M2 cells, or with 10 ml conditioned media prepared by incubating $2x10^5$ of either CHO-TGFα or M2 cells for 25 min in assay medium. To simulate conditions of DNA mediated cell assembly, the same amount of cells were mixed together in 10 ml assay medium and pelleted by centrifugation to force cell-cell contacts.

The respective integrated fluorescence intensities are shown in Figure 24. As expected, 32D-EGFR cells pelleted together which CHO-TGFα cells had the highest EGFR activation level. Co-cultured cells incubated without pelleting exhibited lower activation levels, similar to 32D-EGFR cells incubated in CHO-TGFα conditioned medium. Activation levels were generally higher in samples with CHO-TGFα compared to M2 cells. The juxtacrine signaling portion was estimated by calculating the factor of activation levels of pelleted samples to the respective conditioned medium samples. This results in the ratios 2.20 for CHO-TGFα and 1.46 for M2 cells. This favors the use of CHO-TGFα cells for further experiments.

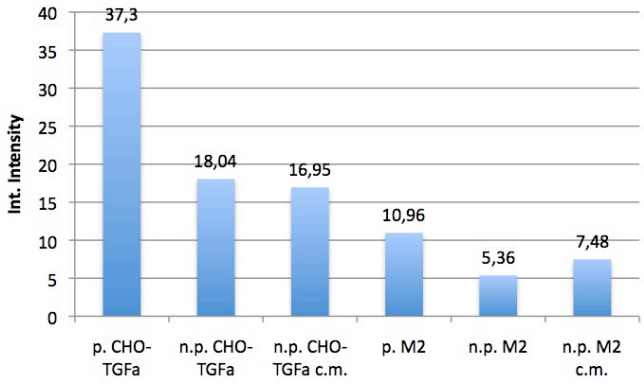

Figure 24. Activation levels of 32D-EGFR cells after stimulation under different conditions. 32D-EGFR cells were mixed with CHO-TGFα cells and pelleted (p.) by centrifugation or without pelleting (n.p.). A third condition was incubation in CHO-TGFα 25 minutes conditioned medium (c.m.). Cells were lysed after 25 minutes of incubation. The same procedure was done with M2 instead of CHO-TGFα cells.

Interestingly, EGFR activation mediated by M2 conditioned medium was higher than when co-culturing 32D-EGFR and M2 cells. This was unanticipated but may suggest that the mutation in M2 cells inactivating TACE does not entirely disrupt the ability of CHO cells to cleave TGFα from the cell surface. On the other hand it was expected that EGFR activation in the presence of TGFα expressing cells would generally lead to a higher level of activation than stimulation with conditioned medium alone, as seen in the co-culture with CHO-TGFα cells. This

difference may be attributed to the gradual increase of TGFα in the medium, reaching a maximum concentration at the end of the experiment. 32D-EGFR cells cultured in conditioned medium, on the other hand, are exposed to the full final concentration of TGFα from the beginning of the experiment. One explanation for the differing levels of activation between M2 co-culture and conditioned media may come from the characteristics of the EGFR activation curves. Cells stimulated by recombinant soluble TGFα (comparable to the effect of conditioned medium) reach a maximum level of activation after about 20 minutes, whereas in co-culture conditions this time point is shifted to about 50 minutes. As cells were lysed after 25 minutes, a higher EGFR activation level of M2 conditioned medium may be explained due to the slower initial rate of activation by the juxtacrine pathway. This discrepancy was not seen when CHO-TGFα cells were used but the difference between levels when not pelleted and incubated in conditioned medium is only small and can reflect a measurement error. These results indicate that incubation of 32D-EGFR cells in conditioned medium is not a perfect control for paracrine signaling.

4.3 DNA-Mediated Cell Assembly

Prior to confirming the capacity of DNA programmed cell assembly to create 3D structures of CHO-TGFα and 32D-EGFR cells, cells were labeled with NHS-DNA and the labeling efficiency was measured in MESF units (molecules of equivalent soluble fluorochrome) using the Quantum FITC-5 MESF beads (Bangs Laboratories). Labeled cells were hybridized with a complementary fluorescent probe and analyzed on a flow cytometer together with unlabeled cells (Figure 25 A-C). Fluorescent bead populations were mixed while blank beads were measured separately (Figure 25 D). Median values were determined and the difference between fluorescent hybridized and non-fluorescent cells was entered into a lot specific excel worksheet downloaded from the Bang Laboratories' website[1]. The results are shown in Table 1. MESF values above $1x10^6$ is considered more than sufficient for cell assembly experiments. The lower value of 32D cells is not surprising considering the smaller size of this cell type and the density of DNA oligomers is presumably the same or even higher relative to CHO-TGFα cells.

[1] http://www.bangslabs.com/

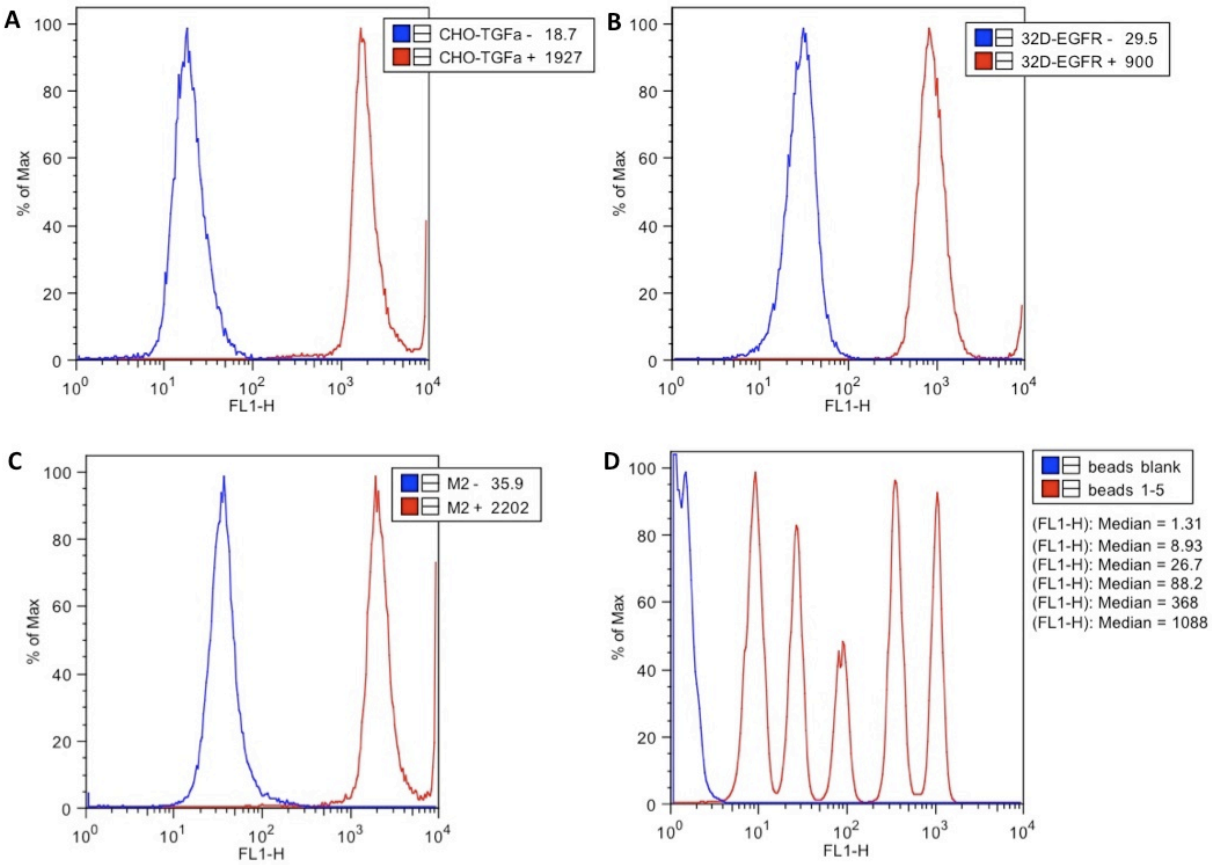

Figure 25. Flow cytometer analysis of labeling efficiency of CHO-TGFα (A), 32D-EGFR (B) and M2 (C) cells. Numbers next to the names indicate median values. Analysis of fluorescent beads which were used as standards is shown in (D) including median values of the peaks. Fluorescent intensities of events measured with channel FL1 are shown as a histogram.

Table 1. MESF values of CHO-TGF, 32D-EGFR, and M2 cells.

Name	difference in median fluorescence	MESF
CHO-TGFα	1908.3	1.974,474
32D-EGFR	870.5	896,408
M2	2166.1	2.242,277

For cell assembly experiments, CHO-TGFα cells were stained with CellTrace DDAO-SE far red dye, 32D-EGFR cells with CellTracker CMFDA green dye (Invitrogen) for 20 minutes in serum free media and in the presence of 2 μM dye. Cells were labeled with 20-mers comprising five repeats of the sequences CAGT or ACTG. Cells were then mixed together at a 1:100 ratio (CHO to 32D) to achieve defined 3D structures as shown in Figure 26. False color fluorescence microscopy of assembled cells. CHO-TGFα cells were stained far red with DDAO-SE, 32D-EGFR cells were stained green with CMFDA. Cells were mixed together at a 1:100 ratio to achieve this defined 3D structure.. A 1:100 mixture of cells functionalized with the same

oligonucleotides were used as a negative control. No cell assemblies could be found by fluorescence microscopy (data not shown).

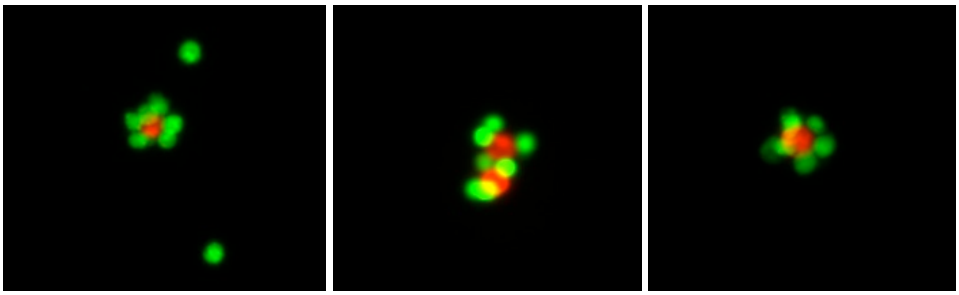

Figure 26. False color fluorescence microscopy of assembled cells. CHO-TGFα cells were stained far red with DDAO-SE, 32D-EGFR cells were stained green with CMFDA. Cells were mixed together at a 1:100 ratio to achieve this defined 3D structure.

Assembled structures where then analyzed by flow cytometry. The fluorescent channels FL1 (green) and FL4 (far red) were adjusted to cleanly resolve the red and green populations (Figure 27 A and B). Events are shown in a scatter plot with channel FL1 on the x-axis and channel FL4 on the y-axis in Figure 27 C-F. Figure 27 C shows far red cells fluorescing at an intensity of about 200 (compare Figure 27 B) in the FL4 channel but do not fluoresce in the FL1 channel. Most cells cannot be seen as they are situated on the y-axis, as the FL1 channel was adjusted in a way that leaves some space at the right end side for assembled structures. Figure 27 D shows green 32D-EGFR cells only. Green cells are situated at an intensity value between 1000 and 2000 of channel FL1 and between 0.4 and 3 on channel FL4. A population named 32D-EGFR green unknown was always visible, also in previous experiments. The 0.15% far red CHO-TGFα cells are contamination due to some far red CHO cells remaining in the flow cytometer after the previous measurement. Figure 27 E shows the analysis of a mix of CHO-TGFα and 32D-EGFR cells labeled with mismatched DNA oligomers (both labeled with 5x ACTG). Only very few events can be found in the "assembled" area.

The flow cytometer results of cells labeled with matched DNA oligonucleotides is depicted in Figure 27 F. Almost all single CHO-TGFα are assembled with green 32D-EGFR cells and can now be found in the region labeled "assembled". The median far red fluorescence associated with the population is between 100 and 200, consistent with a single CHO cell present in each structure. The median green fluorescence associated with the population is 8000, 8-fold higher than individual 32D cells alone. This indicates a median structure of 1 CHO cell associate with 8 32D cells. Assembly efficiency can be calculated by utilizing the percentage values situated below the area names, suggesting an efficiency of 0.42/(0.42+0.017)x100=96.1%.

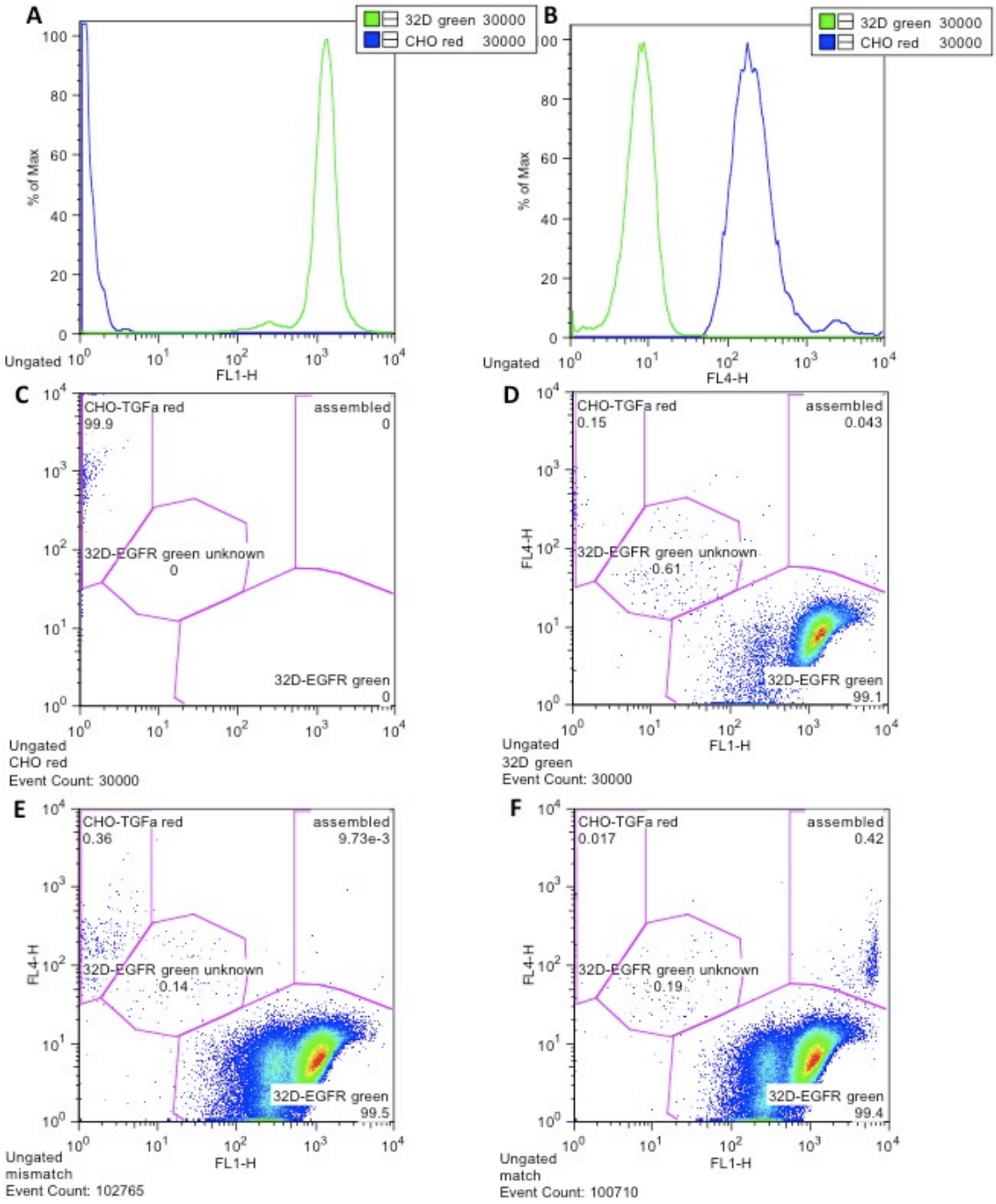

Figure 27. Flow cytometer analysis of assembled CHO-TGFα and 32D-EGFR cells.

4.4 EGFR Activation by DNA Mediated Cell-Cell Contacts

After determining EGFR activation levels, kinetics, and confirming cell assembly mediated by surface DNA oligomers, a final combinatorial experiment was performed. In accordance with the previous experiments described above, a timeframe of one hour was chosen to achieve a high activation level in co-culture conditions. A 1:8 (CHO-TGFa to 32D-

EGFR) cell ratio was chosen as epifluorescence microscopy and flow cytometry indicated space for 6 to 10 32D-EGFR cells surrounding CHO-TGFa cells. A dilute cell concentration of approximately $1x10^5$/ml was chosen to minimize EGFR activation due to soluble TGFa. All methods were applied as described in chapter 3.

In brief, four times 1 hr CHO- TGFα conditioned medium was prepared with $1.25x10^5$ cells in 10 ml assay medium each and stored on ice until use. CHO- TGFα cells labelled or unlabeled were washed three times in ice cold PBS supplemented with 1% FBS (PBS-FBS). All cells were counted and PBS-FBS was pipetted into 1.5 ml tubes to achieve a final concentration of $1x10^6$/ml. $1.25x10^5$ CHO cells were added first, followed by $1x10^6$ 32D-EGFR cells. All samples were spun down (all spins were performed at 900 g for 3 min) at 4°C to achieve DNA-mediated cell assembly and to ensure uniform treatment of all samples. Pelleted cells were then resuspended and added to 10 ml prewarmed 37°C assay medium or CHO- TGFα conditioned medium in 15 ml Falcon tubes for 1 hr. The samples "pelleted" were spun down and incubated in a 37° water bath. All other samples were put onto a rotating wheel in a 37°C incubator. TGFα was added to a final concentrations of 20 ng/ml for the respective control sample. After 1 hr of incubation, all samples were put on ice, cooled down for 5 min, spun down at 4°C and lysed. 60 µg total protein was loaded onto denaturing acrylamide gel and immunoblotting was performed as described.

Figure 28 depicts EGFR activation levels of 32D-EGFR cells incubated for 1 hr under different conditions. The first sample represents co-cultured 32D-EGFR and CHO-TGFα cells which had been functionalized with complementary oligonucleotides. The activation level is similar to the second condition in which cell-cell contact was achieved by centrifugation. In the third condition, named "not pelleted" cells were added in suspension to the assay medium. In the next sample 32D-EGFR cells were incubated with 1 hr-CHO- TGFα conditioned medium. Together with the previous sample (not pelleted), this condition was intended to account for the paracrine portion of EGFR activation. The cell density of CHO-TGFα cells was $1.25x10^4$/ml and $1x10^5$/ml for 32D-EGFR cells. Under such conditions the likelihood of enough CHO-TGFα cells touching 32D-EGFR cells and thereby leading to detectable amounts of phosphorylated EGFR by the juxtacrine mode of activation is very unlikely. Therefore only the more abundant soluble TGFα ligands can bind to EGF receptors, constituting the paracrine mode of activation. However, the intensity of paracrine signaling is presumably much higher under conditions of close proximity of sender and receiver cells. For that reason, the level of EGFR activation of the not pelleted sample only very roughly emulates the paracrine level of activation when cells are in contact with each other, as it is the case with assembled and pelleted cells. For the same reason, the conditioned medium control should be interpreted with caution as well. Additionally the different kinetics of stimulating 32D-EGFR cells with soluble TGFα or conditioned medium versus in co-culture conditions have to be taken into account, as described in chapter 4.2 for conditioned medium of M2 cells.

Samples 5 to 7 are similar to samples 1 to 3, but with incubation in CHO-TGFα conditioned medium instead of in assay medium. The aim was to look for optimal conditions to achieve a high signal to noise ratio. This time the pelleted condition showed higher activation levels than when cells were assembled by DNA labeling.

Samples 8 and 9 represent 32D-EGFR cells incubated with the vector only CHO-pB cell line. Those samples account for the general background level probably caused by secretion of low levels of different growth factors by CHO cells which can activate EGFR. Interestingly these levels are comparable to the paracrine controls (samples 3 and 4), suggesting a very low contribution of secreted TGFα on activation of 32D-EGFR cells in suspension. The 32-EGFR(-) sample cells without EGFR stimulation. 32D-EGFR cells stimulated with 20 ng/ml TGFα and A 431 cells were used as positive controls.

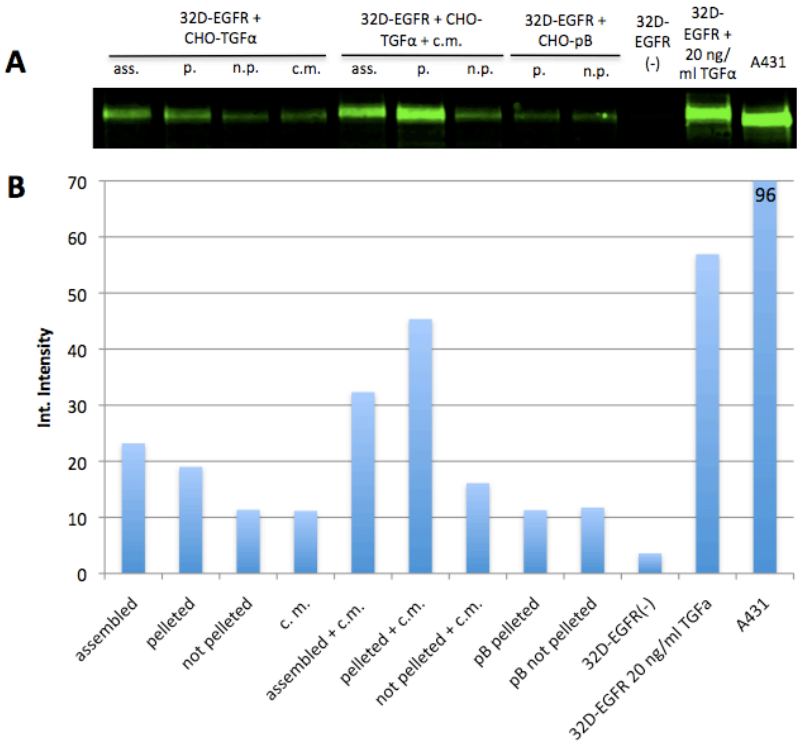

Figure 28. EGFR activation levels of 32D-EGFR cells incubated for 1 hr under different conditions. (A) Quantitative Western blot analyzed with the Licor system. (B) Integrated fluorescence intensities of the bands are depicted as a histogram.

In order to confirm the results presented above, this experiment will be repeated two more times to account for statistical spread caused by differences in cell counting, pipetting, protein transfer onto the blotting membrane, and other possible procedural variables. This will also determine the significance of the results. Similarly, more differential controls will be added. A condition with DNA-labeled 32D-EGFR cells stimulated with soluble TGFα will give information about possible receptor activation inhibition caused by binding of DNA-NHS-conjugates to lysines on the receptor. A condition with 32D-EGFR cells combined with DNA-labeled CHO-TGFα cells in turn can account for inhibition of activation due to binding of DNA strands to the TGFα ligand. In combination with controls described above, a sample with both

cell types labeled with mismatched DNA strands mechanically brought together by centrifugation will provide insights into possible signaling inhibition caused by spatial restrictions due to DNA strands on the cell surface.

5 Concluding Remarks

In summary, I reconstituted the paracrine and juxtacrine TGFα-EGFR signaling pathway by assembling two different kinds of cell types using DNA programmed cell assembly. I demonstrated that ligand-receptor binding is not inhibited by covalently linking NHS-DNA conjugates to cell surface proteins and that levels of EGFR activation induced by DNA-programmed assembly are similar to those when cell-cell contacts are mechanically initiated by centrifugation. Previous studies suggest that high level of activation mediated by cell-cell contacts is likely a consequence of the juxtacrine signaling [6, 52]. Control experiments in which 32D-EGFR cells were incubated in CHO-TGFα conditioned medium or in co-culture conditions without achieving cell-cell contacts support but do not prove this hypothesis. Nevertheless, this work provides a foundation for future studies focusing on the differentiation between the juxtacrine and the paracrine portion of signaling pathways that comprise both modes of cell communication.

It has been reported that when co-cultured with a murine stromal bone marrow cell line retrovirally transformed to express TGFα, 32D-EGFR cells can attach to the cell monolayer and form foci of flattened adherent cells [27]. This suggests that the hematopoietic progenitor 32D cells have transitioned into a more differentiated state. These observations should motivate future functional assays with CHO-TGFα and 32D-EGFR cells in 3D co-culture systems. As shown in chapter 4.3, defined cell structures can be identified by flow cytometry when cells are stained with different fluorescent dyes. Fluorescence-activated cell sorting can therefore be applied to isolate only assembled cell clusters. Cells sorted into matrices allowing formation of 3D structures, for example matrigel or hydrogel, could then freely form different types of microtissues. Depending on parameters such as the ratio between sender and receiver cells, the size of the initial structure, and the type of the signaling pathway one might expect diverging behaviors of the resulting tissues.

Another possibility to achieve defined 3D structures by applying DNA templated tissue synthesis involves the attachment of a DNA labeled TGFα expressing cell to a surface with spots functionalized with complementary oligonucleotides. In the Gartner lab, DNA can be spotted onto surfaces with a diameter of less than 10 μm, comprising space for a single cell on each spot. In a second step, 32D-EGFR cells can be attached to the CHO-TGFα or M2 cells. Cell structures formed on a surface in this way can be lifted by letting low melting agarose containing DNAse solidify on the cells and transferring them onto a growth matrix that allows formation and maintenance of 3D multicellular structures. Cell morphology, motility, survival, or growth can then be investigated with or without addition of IL-3 or other growth factors. A major advantage of this technique is that it allows placement of assembled cells at defined locations on a grid within a 3D growth matrix, thereby enabling examination of single events in a defined spatial relationship over an extended period of time. Currently, no other means of achieving this are currently available.

It would be interesting to compare proliferation and morphology of 32D-EGFR microtissues in a system like the ones mentioned where they form assembled structures with CHO-TGFα or M2 cells, capable and incapable, respectively, of TGFα shedding. By that means, differences in juxtacrine versus paracrine signaling could be investigated. Similarly, TGFα and EGFR expressing cells could be placed at precisely defined distances from each other without actually making cell-cell contacts but residing in close proximity. This would allow low levels of paracrine signaling via TGFα shedding to be distinguished from bonafide juxtacrine signaling which is absolutely reliant on cell-cell contact.

6 References

1. Gartner, Z.J. and C.R. Bertozzi, *Programmed assembly of 3-dimensional microtissues with defined cellular connectivity.* Proc Natl Acad Sci U S A, 2009. **106**(12): p. 4606-10.
2. Hebner, C., V.M. Weaver, and J. Debnath, *Modeling morphogenesis and oncogenesis in three-dimensional breast epithelial cultures.* Annu Rev Pathol, 2008. **3**: p. 313-39.
3. Hynes, N.E. and H.A. Lane, *ERBB receptors and cancer: the complexity of targeted inhibitors.* Nat Rev Cancer, 2005. **5**(5): p. 341-54.
4. Humphreys, R.C. and L. Hennighausen, *Transforming growth factor alpha and mouse models of human breast cancer.* Oncogene, 2000. **19**(8): p. 1085-91.
5. Yang, H., D. Jiang, W. Li, J. Liang, L.E. Gentry, and M.G. Brattain, *Defective cleavage of membrane bound TGFalpha leads to enhanced activation of the EGF receptor in malignant cells.* Oncogene, 2000. **19**(15): p. 1901-14.
6. Shi, W., H. Fan, L. Shum, and R. Derynck, *The tetraspanin CD9 associates with transmembrane TGF-alpha and regulates TGF-alpha-induced EGF receptor activation and cell proliferation.* J Cell Biol, 2000. **148**(3): p. 591-602.
7. Miyake, M., K. Nakano, S.I. Itoi, T. Koh, and T. Taki, *Motility-related protein-1 (MRP-1/CD9) reduction as a factor of poor prognosis in breast cancer.* Cancer Res, 1996. **56**(6): p. 1244-9.
8. Hsiao, S.C., B.J. Shum, H. Onoe, E.S. Douglas, Z.J. Gartner, R.A. Mathies, C.R. Bertozzi, and M.B. Francis, *Direct cell surface modification with DNA for the capture of primary cells and the investigation of myotube formation on defined patterns.* Langmuir, 2009. **25**(12): p. 6985-91.
9. Baskin, J.M., J.A. Prescher, S.T. Laughlin, N.J. Agard, P.V. Chang, I.A. Miller, A. Lo, J.A. Codelli, and C.R. Bertozzi, *Copper-free click chemistry for dynamic in vivo imaging.* Proc Natl Acad Sci U S A, 2007. **104**(43): p. 16793-7.
10. Codelli, J.A., J.M. Baskin, N.J. Agard, and C.R. Bertozzi, *Second-generation difluorinated cyclooctynes for copper-free click chemistry.* J Am Chem Soc, 2008. **130**(34): p. 11486-93.
11. Kolb, H.C., M.G. Finn, and K.B. Sharpless, *Click Chemistry: Diverse Chemical Function from a Few Good Reactions.* Angew Chem Int Ed Engl, 2001. **40**(11): p. 2004-2021.
12. Kumar, V., S.A. Bustin, and I.A. McKay, *Transforming growth factor alpha.* Cell Biol Int, 1995. **19**(5): p. 373-88.
13. Bringman, T.S., P.B. Lindquist, and R. Derynck, *Different transforming growth factor-alpha species are derived from a glycosylated and palmitoylated transmembrane precursor.* Cell, 1987. **48**(3): p. 429-40.
14. Citri, A. and Y. Yarden, *EGF-ERBB signalling: towards the systems level.* Nat Rev Mol Cell Biol, 2006. **7**(7): p. 505-16.
15. Song, J.I. and J.R. Grandis, *STAT signaling in head and neck cancer.* Oncogene, 2000. **19**(21): p. 2489-95.
16. Cohen, S., *Isolation of a mouse submaxillary gland protein accelerating incisor eruption and eyelid opening in the new-born animal.* J Biol Chem, 1962. **237**: p. 1555-62.
17. Savage, C.R., Jr., T. Inagami, and S. Cohen, *The primary structure of epidermal growth factor.* J Biol Chem, 1972. **247**(23): p. 7612-21.
18. Harris, R.C., E. Chung, and R.J. Coffey, *EGF receptor ligands.* Exp Cell Res, 2003. **284**(1): p. 2-13.
19. Massague, J., *Transforming growth factor-alpha. A model for membrane-anchored growth factors.* J Biol Chem, 1990. **265**(35): p. 21393-6.

20. Rebay, I., R.J. Fleming, R.G. Fehon, L. Cherbas, P. Cherbas, and S. Artavanis-Tsakonas, *Specific EGF repeats of Notch mediate interactions with Delta and Serrate: implications for Notch as a multifunctional receptor.* Cell, 1991. **67**(4): p. 687-99.

21. Brachmann, R., P.B. Lindquist, M. Nagashima, W. Kohr, T. Lipari, M. Napier, and R. Derynck, *Transmembrane TGF-alpha precursors activate EGF/TGF-alpha receptors.* Cell, 1989. **56**(4): p. 691-700.

22. Derynck, R., *The physiology of transforming growth factor-alpha.* Adv Cancer Res, 1992. **58**: p. 27-52.

23. Xu, P. and R. Derynck, *Direct activation of TACE-mediated ectodomain shedding by p38 MAP kinase regulates EGF receptor-dependent cell proliferation.* Mol Cell, 2010. **37**(4): p. 551-66.

24. Luetteke, N.C., G.K. Michalopoulos, J. Teixido, R. Gilmore, J. Massague, and D.C. Lee, *Characterization of high molecular weight transforming growth factor alpha produced by rat hepatocellular carcinoma cells.* Biochemistry, 1988. **27**(17): p. 6487-94.

25. Ignotz, R.A., B. Kelly, R.J. Davis, and J. Massague, *Biologically active precursor for transforming growth factor type alpha, released by retrovirally transformed cells.* Proc Natl Acad Sci U S A, 1986. **83**(17): p. 6307-11.

26. Wong, S.T., L.F. Winchell, B.K. McCune, H.S. Earp, J. Teixido, J. Massague, B. Herman, and D.C. Lee, *The TGF-alpha precursor expressed on the cell surface binds to the EGF receptor on adjacent cells, leading to signal transduction.* Cell, 1989. **56**(3): p. 495-506.

27. Anklesaria, P., J. Teixido, M. Laiho, J.H. Pierce, J.S. Greenberger, and J. Massague, *Cell-cell adhesion mediated by binding of membrane-anchored transforming growth factor alpha to epidermal growth factor receptors promotes cell proliferation.* Proc Natl Acad Sci U S A, 1990. **87**(9): p. 3289-93.

28. Lemmon, M.A., *Ligand-induced ErbB receptor dimerization.* Exp Cell Res, 2009. **315**(4): p. 638-48.

29. Burgess, A.W., H.S. Cho, C. Eigenbrot, K.M. Ferguson, T.P. Garrett, D.J. Leahy, M.A. Lemmon, M.X. Sliwkowski, C.W. Ward, and S. Yokoyama, *An open-and-shut case? Recent insights into the activation of EGF/ErbB receptors.* Mol Cell, 2003. **12**(3): p. 541-52.

30. Lemmon, M.A. and J. Schlessinger, *Cell signaling by receptor tyrosine kinases.* Cell, 2010. **141**(7): p. 1117-34.

31. Flynn, J.F., C. Wong, and J.M. Wu, *Anti-EGFR Therapy: Mechanism and Advances in Clinical Efficacy in Breast Cancer.* J Oncol, 2009. **2009**: p. 526963.

32. Ogiso, H., R. Ishitani, O. Nureki, S. Fukai, M. Yamanaka, J.H. Kim, K. Saito, A. Sakamoto, M. Inoue, M. Shirouzu, and S. Yokoyama, *Crystal structure of the complex of human epidermal growth factor and receptor extracellular domains.* Cell, 2002. **110**(6): p. 775-87.

33. Garrett, T.P., N.M. McKern, M. Lou, T.C. Elleman, T.E. Adams, G.O. Lovrecz, H.J. Zhu, F. Walker, M.J. Frenkel, P.A. Hoyne, R.N. Jorissen, E.C. Nice, A.W. Burgess, and C.W. Ward, *Crystal structure of a truncated epidermal growth factor receptor extracellular domain bound to transforming growth factor alpha.* Cell, 2002. **110**(6): p. 763-73.

34. Dawson, J.P., M.B. Berger, C.C. Lin, J. Schlessinger, M.A. Lemmon, and K.M. Ferguson, *Epidermal growth factor receptor dimerization and activation require ligand-induced conformational changes in the dimer interface.* Mol Cell Biol, 2005. **25**(17): p. 7734-42.

35. Schlessinger, J., *Ligand-induced, receptor-mediated dimerization and activation of EGF receptor.* Cell, 2002. **110**(6): p. 669-72.

36. Ferguson, K.M., M.B. Berger, J.M. Mendrola, H.S. Cho, D.J. Leahy, and M.A. Lemmon, *EGF activates its receptor by removing interactions that autoinhibit ectodomain dimerization.* Mol Cell, 2003. **11**(2): p. 507-17.

37. Schlessinger, J., *Signal transduction. Autoinhibition control.* Science, 2003. **300**(5620): p. 750-2.

38. Mattoon, D., P. Klein, M.A. Lemmon, I. Lax, and J. Schlessinger, *The tethered configuration of the EGF receptor extracellular domain exerts only a limited control of receptor function.* Proc Natl Acad Sci U S A, 2004. **101**(4): p. 923-8.

39. Ozcan, F., P. Klein, M.A. Lemmon, I. Lax, and J. Schlessinger, *On the nature of low- and high-affinity EGF receptors on living cells.* Proc Natl Acad Sci U S A, 2006. **103**(15): p. 5735-40.

40. Lammerts van Bueren, J.J., W.K. Bleeker, A. Brannstrom, A. von Euler, M. Jansson, M. Peipp, T. Schneider-Merck, T. Valerius, J.G. van de Winkel, and P.W. Parren, *The antibody zalutumumab inhibits epidermal growth factor receptor signaling by limiting intra- and intermolecular flexibility.* Proc Natl Acad Sci U S A, 2008. **105**(16): p. 6109-14.

41. McLaughlin, S., S.O. Smith, M.J. Hayman, and D. Murray, *An electrostatic engine model for autoinhibition and activation of the epidermal growth factor receptor (EGFR/ErbB) family.* J Gen Physiol, 2005. **126**(1): p. 41-53.

42. Zhang, X., J. Gureasko, K. Shen, P.A. Cole, and J. Kuriyan, *An allosteric mechanism for activation of the kinase domain of epidermal growth factor receptor.* Cell, 2006. **125**(6): p. 1137-49.

43. Jura, N., N.F. Endres, K. Engel, S. Deindl, R. Das, M.H. Lamers, D.E. Wemmer, X. Zhang, and J. Kuriyan, *Mechanism for activation of the EGF receptor catalytic domain by the juxtamembrane segment.* Cell, 2009. **137**(7): p. 1293-307.

44. Emlet, D.R., D.K. Moscatello, L.B. Ludlow, and A.J. Wong, *Subsets of epidermal growth factor receptors during activation and endocytosis.* J Biol Chem, 1997. **272**(7): p. 4079-86.

45. Zwick, E., P.O. Hackel, N. Prenzel, and A. Ullrich, *The EGF receptor as central transducer of heterologous signalling systems.* Trends Pharmacol Sci, 1999. **20**(10): p. 408-12.

46. Hackel, P.O., E. Zwick, N. Prenzel, and A. Ullrich, *Epidermal growth factor receptors: critical mediators of multiple receptor pathways.* Curr Opin Cell Biol, 1999. **11**(2): p. 184-9.

47. Wiley, H.S., J.J. Herbst, B.J. Walsh, D.A. Lauffenburger, M.G. Rosenfeld, and G.N. Gill, *The role of tyrosine kinase activity in endocytosis, compartmentation, and down-regulation of the epidermal growth factor receptor.* J Biol Chem, 1991. **266**(17): p. 11083-94.

48. Sorkin, A. and L.K. Goh, *Endocytosis and intracellular trafficking of ErbBs.* Exp Cell Res, 2009. **315**(4): p. 683-96.

49. Singh, A.B. and R.C. Harris, *Autocrine, paracrine and juxtacrine signaling by EGFR ligands.* Cell Signal, 2005. **17**(10): p. 1183-93.

50. Takemura, T., S. Hino, M. Okada, Y. Murata, H. Yanagida, M. Ikeda, K. Yoshioka, and R.C. Harris, *Role of membrane-bound heparin-binding epidermal growth factor-like growth factor (HB-EGF) in renal epithelial cell branching.* Kidney Int, 2002. **61**(6): p. 1968-79.

51. Singh, A.B., T. Tsukada, R. Zent, and R.C. Harris, *Membrane-associated HB-EGF modulates HGF-induced cellular responses in MDCK cells.* J Cell Sci, 2004. **117**(Pt 8): p. 1365-79.

52. Imhof, I., W.J. Gasper, and R. Derynck, *Association of tetraspanin CD9 with transmembrane TGF{alpha} confers alterations in cell-surface presentation of TGF{alpha} and cytoskeletal organization.* J Cell Sci, 2008. **121**(Pt 13): p. 2265-74.

53. Gartel, A.L. and S.K. Radhakrishnan, *Lost in transcription: p21 repression, mechanisms, and consequences.* Cancer Res, 2005. **65**(10): p. 3980-5.

54. Fan, H. and R. Derynck, *Ectodomain shedding of TGF-alpha and other transmembrane proteins is induced by receptor tyrosine kinase activation and MAP kinase signaling cascades.* EMBO J, 1999. **18**(24): p. 6962-72.

55. Morgenstern, J.P. and H. Land, *Advanced mammalian gene transfer: high titre retroviral vectors with multiple drug selection markers and a complementary helper-free packaging cell line.* Nucleic Acids Res, 1990. **18**(12): p. 3587-96.

56. Giard, D.J., S.A. Aaronson, G.J. Todaro, P. Arnstein, J.H. Kersey, H. Dosik, and W.P. Parks, *In vitro cultivation of human tumors: establishment of cell lines derived from a series of solid tumors.* J Natl Cancer Inst, 1973. **51**(5): p. 1417-23.

57. Li, X. and H. Fan, *Loss of ectodomain shedding due to mutations in the metalloprotease and cysteine-rich/disintegrin domains of the tumor necrosis factor-alpha converting enzyme (TACE).* J Biol Chem, 2004. **279**(26): p. 27365-75.

58. Pierce, J.H., M. Ruggiero, T.P. Fleming, P.P. Di Fiore, J.S. Greenberger, L. Varticovski, J. Schlessinger, G. Rovera, and S.A. Aaronson, *Signal transduction through the EGF receptor transfected in IL-3-dependent hematopoietic cells.* Science, 1988. **239**(4840): p. 628-31.

59. Wiley, H.S., *Anomalous binding of epidermal growth factor to A431 cells is due to the effect of high receptor densities and a saturable endocytic system.* J Cell Biol, 1988. **107**(2): p. 801-10.

60. Lund, K.A., L.K. Opresko, C. Starbuck, B.J. Walsh, and H.S. Wiley, *Quantitative analysis of the endocytic system involved in hormone-induced receptor internalization.* J Biol Chem, 1990. **265**(26): p. 15713-23.

7 Table of Figures

8 List of Tables